Paleoceanography and Paleoclimatology

RESEARCH ARTICLE
10.1029/2021PA004243

Wetter Subtropics Lead to Reduced Pliocene Coastal Upwelling

Minmin Fu[1], Mark A. Cane[2], Peter Molnar[3,4], and Eli Tziperman[1,5]

[1]Department of Earth and Planetary Sciences, Harvard University, Cambridge, MA, USA, [2]Lamont-Doherty Earth Observatory, Columbia University, Palisades, NY, USA, [3]Department of Geological Sciences, University of Colorado Boulder, Boulder, CO, USA, [4]Cooperative Institute for Research in Environmental Sciences, University of Colorado Boulder, Boulder, CO, USA, [5]School of Engineering and Applied Sciences, Harvard University, Cambridge, MA, USA

Key Points:

- Proxy evidence indicates wetter subtropical continents and dramatically warmer sea surface temperatures (SSTs) at coastal upwelling sites during the Pliocene
- Prescribing idealized wetter land conditions reduces land-sea pressure gradients and weakens alongshore upwelling-favorable winds
- This weakening leads to strong reductions in upwelling-favorable wind events, helping to explain Pliocene SST warmth

Supporting Information:

Supporting Information may be found in the online version of this article.

Correspondence to:

M. Fu,
mjfu@g.harvard.edu

Citation:

Fu, M., Cane, M. A., Molnar, P., & Tziperman, E. (2021). Wetter subtropics lead to reduced Pliocene coastal upwelling. *Paleoceanography and Paleoclimatology*, *36*, e2021PA004243. https://doi.org/10.1029/2021PA004243

Received 11 FEB 2021
Accepted 30 SEP 2021

Abstract Current global warming scenarios suggest surface temperatures may attain warmth last seen during periods of the early-to mid-Pliocene (5.3–3 Ma). Pliocene proxy reconstructions suggest sea surface temperatures 3–9°C warmer than today along midlatitude coastal upwelling sites. Recent climate modeling efforts focused on the mid-Piacenzian period showed a good model-data fit over midlatitude upwelling regions, but did not attempt to reproduce proxy records of early-Pliocene warmth. Evidence also suggests that subtropical continents were wetter then; we show that warm coastal SSTs can be explained via such wetter land conditions near the upwelling sites. Using a global atmospheric model, we show that introducing idealized wetter conditions over subtropical continents leads to reductions in upwelling-favorable wind events by weakening the land-sea surface pressure gradient. The resulting weaker coastal upwelling of cold deep water can help explain the inferred warm coastal temperatures.

1. Introduction

One particularly intriguing feature of proxy reconstructions of Pliocene sea surface temperatures (SSTs) is the dramatically higher temperatures inferred at several midlatitude coastal upwelling sites. Midlatitude coastal upwelling today occurs along the eastern boundaries of the Atlantic and Pacific basins and results in narrow strips of cold SST extending 10–50 km off the coasts (Allen, 1980; Enriquez & Friehe, 1995; Hurlburt & Thompson, 1973; Renault et al., 2012; Small et al., 2015). Although the 3°C–4°C warmer global-mean Pliocene surface temperature (Dowsett et al., 2011, 2013; McClymont et al., 2020; O'Brien et al., 2014; Tierney et al., 2019) accounts for some Pliocene warmth at these upwelling sites, the fact that SSTs at those sites were 3°C–9°C warmer than present day suggests that the narrow strips of cold upwelling at those sites today operated differently during the early-to mid-Pliocene (Brierley et al., 2009; Dekens et al., 2007; Herbert & Schuffert, 1998; Marlow et al., 2000).

Several mechanisms have been proposed to explain the anomalous warmth at coastal upwelling sites and the possible reduction in SST difference between the eastern and western equatorial Pacific, sometimes referred to as a "permanent El Niño" (Fedorov et al., 2006; K. T. Lawrence et al., 2006; Molnar & Cane, 2002, 2007; Philander & Fedorov, 2003; Ravelo et al., 2006). One suggestion is that during the Pliocene, a deeper thermocline meant cold waters remained below the level that could be brought to the surface by upwelling winds (Boccaletti et al., 2004; Philander & Fedorov, 2003). Proposed mechanisms for such a deeper thermocline include a response to the large scale meridional temperature distribution (Boccaletti et al., 2004), the closure of the Central American Seaway (Steph et al., 2010), or changes in tropical cyclone frequency leading to increases in vertical ocean mixing (Fedorov et al., 2010). However, these mechanisms do not explain the observations satisfactorily (Fedorov et al., 2013).

The existence of a permanent El Niño state has been debated. While some studies suggested its existence in the early Pliocene (Brierley et al., 2009, 2015; Ravelo et al., 2006, 2014; Wara et al., 2005; Wycech et al., 2020), others debated that (O'Brien et al., 2014; Zhang et al., 2014). For the mid-Piacenzian, which has been suggested as a closer analog of near future warming, some studies suggested the existence of a permanent El Niño state (Brierley et al., 2009, 2015; Ravelo et al., 2006, 2014; Wara et al., 2005; Wycech et al., 2020), and some, again, disagreed (O'Brien et al., 2014; Tierney et al., 2019; Zhang et al., 2014). The subtropical upwelling zones considered in this study, where SSTs are below 30°C, are expected to be insensitive to alkenone calibration differences. While SST reconstructions by both Tierney et al. (2019), and PRISM (Dowsett

& Robinson, 2009) do not show large midlatitude upwelling site warming, their period of study is later than the point measurements mentioned above.

An alternative explanation for the warm SSTs at Pliocene upwelling sites is that the upwelling-favorable winds around the coastal upwelling sites may have been weaker. Ocean modeling of the effect of ocean stratification and surface wind stresses on coastal upwelling indicates that significantly weaker winds are likely needed to explain the anomalous warmth (Miller & Tziperman, 2017). Modern upwelling-favorable mean winds near midlatitude upwelling sites are related to the subtropical highs, regions of high surface pressure over oceans at around 30°N and 30°S, which result in alongshore wind stress (AWS) parallel to shore. One mechanism for changes to these upwelling-favorable winds is through weaker subtropical highs and weaker associated anticyclonic surface winds (Arnold & Tziperman, 2016), possibly due to a decrease in the strength of Hadley cell subsidence over the midlatitudes. Another mechanism for changing the large-scale global wind patterns that affect the tropics, a permanent El Niño, and perhaps midlatitude winds is atmospheric superrotation that was proposed to be active during the Pliocene, with westerly or weakened easterly winds near the equator that could have affected the large-scale SST (Arnold et al., 2012; Tziperman & Farrell, 2009).

Another notable feature of Pliocene climate is evidence indicating that the subtropical continents were wetter compared to present day. In much of western North America, for example, generally higher levels of precipitation have been inferred from paleobotanic evidence (Thompson, 1991; Thompson & Fleming, 1996). Sedimentary evidence of large permanent lakes in Colorado (Machette et al., 2013), Southwestern Idaho (Forester, 1991), and the Death Valley region of eastern California (Knott et al., 2008; Knott et al., 2018; G. I. Smith, 1984) indicate Pliocene conditions that were wetter than present-day near the coast as well as further inland. A map summarizing evidence of Pliocene lakes over western North America is included in Figure S1 in Supporting Information S1. Overall, as pointed out in Appendix A and Table A1, the available evidence points towards a global Pliocene climate characterized by wetter subtropical continents with a more ample supply of soil moisture (Burls & Fedorov, 2017; Pound et al., 2014; Salzmann et al., 2008). To explain these wetter conditions, Burls and Fedorov (2017) explored how a different atmospheric circulation could have transported more water to the subtropics.

To explain the marked warming in regions where coastal upwelling occurs today, we consider how moister Pliocene land conditions could have modified the atmospheric circulation and therefore reduced upwelling-favorable wind-events. Upwelling wind-events, characterized by alongshore wind over a threshold of 5 m/s lasting at least 3 days, have been found to be most effective for bringing cold water to the ocean surface (Botsford et al., 2006; Dugdale et al., 2006; García-Reyes & Largier, 2010). We prescribe a range of idealized wetter land conditions over the coastal regions of subtropical continents near four major upwelling sites and study the resulting effects on upwelling winds. We focus on the coastal upwelling systems near the California, Canary, Humboldt, and Benguela Currents, where Pliocene proxy evidence is available from studies done at Ocean Drilling Program (ODP) sites. We show that the resulting changes to upwelling-favorable wind events can help rationalize the inferred early-to mid-Pliocene SST differences at the California (~+8°C, Brierley et al., 2009; Dekens et al., 2007; LaRiviere et al., 2012), Canary (+4.1°C, Herbert & Schuffert, 1998), and Benguela (+9.3°C, Marlow et al., 2000) Currents (where McClymont et al., 2020 found a large model-data mismatch), with the smaller inferred difference at the Humboldt Current (+2.9°C, Dekens et al., 2007) consistent with the global cooling of ~3°C since the Pliocene and the insignificant wind changes that we find there. A recent Pliocene modeling inter-comparison effort (Haywood et al., 2020) focused on 3.19–3.22 Ma, during the mid-Piacenzian, and showed a good fit between the reconstruction of Foley and Dowsett (2019) and model results. However, this data set does not include the above-mentioned proxy observations showing warm upwelling sites in earlier parts of the Pliocene. These warm temperatures during the early Pliocene have yet to be stringently tested with the latest generation of climate models, and it remains to be seen whether proxy records from the early Pliocene can now be resolved in coupled climate models.

Table 1
Summary of Experimental Configurations

Experiment name	Model Configuration
Modern	HadISST, 355 ppm CO_2, modern topography and land types.
PRISM	As in Modern, but with PRISM3 SST and 405 ppm CO_2.
$PRISM_L$	As in PRISM, but using Pliocene land surface types.
$PRISM_{25}$	As in PRISM, but with 25% wetland over subtropical coasts.
$PRISM_{50}$	As in PRISM, but with 50% wetland over subtropical coasts.
$PRISM_{100}$	As in PRISM, but with 100% wetland over subtropical coasts.

2. Methods

2.1. Model Configuration

Our study utilizes atmospheric General Circulation Model (GCM) simulations representing modern conditions (Modern) as well as Pliocene conditions based on data from the PRISM project. Although the PRISM reconstruction specifically targeted the mid-Piacenzian, the objective of this study is to investigate more broadly the warm upwelling site SSTs that characterized the early-to mid-Pliocene (5.3–3 Ma). In addition to a simulation (model experiment PRISM) with prescribed PRISM3 SSTs (Dowsett & Robinson, 2009) and alleged Pliocene CO_2 concentrations (Kürschner et al., 1996; Pagani et al., 2010; Raymo et al., 1996; Seki et al., 2010), simulations with Pliocene vegetation included ($PRISM_L$) or various grid-cell percentages of wetland added near the subtropical coasts (model experiments $PRISM_{25}$, $PRISM_{50}$, & $PRISM_{100}$) are also performed. Our modern experiment uses the merged Hadley Centre Sea Ice and SST data set 1 (HadISST1) and National Oceanic and Atmospheric Administration (NOAA) weekly optimum interpolation SST analysis (Hurrell et al., 2008). This data set represents preindustrial SSTs. For all Pliocene simulations, we use PRISM3 SST data representing mid-Piacenzian SSTs (Dowsett & Robinson, 2009). For those experiments including Pliocene land types, we prescribe PRISM3 biomes (Salzmann et al., 2008) with modern lake and soil distributions, following the methods used in the the Pliocene Model Intercomparison Project (PlioMIP1, Rosenbloom et al., 2013). All Pliocene simulations are forced with an elevated CO_2 level of 405 ppm (as recommended by PlioMIP1, Haywood et al., 2010), while the Modern simulation is forced with a CO_2 level of 355 ppm. A summary of all experimental configurations is provided in Table 1.

Our simulations use the NCAR Community Earth System Model version 1.2.2.1 with the Community Atmosphere Model (CAM) version 5.3 as its atmospheric component (Neale et al., 2012). The land component used is the Community Land Model (CLM) version 4.0 (D. M. Lawrence et al., 2011), and all orbital parameters are set to modern values. In CAM we use the bulk aerosols model with the chemistry package disabled. Topography for all simulations is set to modern values and all simulations are run at a nominal 1 degree resolution (0.9° × 1.25°) with 30 vertical levels. All simulations are run for 80 years, with the first five years discarded to allow for model spin-up. Next, we describe the procedure for prescribing wetlands near the coasts.

2.2. Prescribed Wetlands

To introduce wetter land conditions consistent with the paleobotanical and paleohydrologic evidence, we prescribe wetland along the subtropical coasts of the American and African continents, near the position of four relevant ODP sites. In the CLM, wetlands are defined as columns of water with 100% surface moisture availability, but with interactive rather than prescribed temperatures. This enables wetlands to gain and lose heat according to local energy balance. For the California Current near ODP Site 1014, wetland is added from 20°N–50°N and 10° longitude inland from the western continental boundary. For the Humboldt Current near ODP Site 1237, wetland is added from 5°S–40°S and 4° longitude inland. For the Canary Current near ODP Site 958, wetland is added from 10°N–40°N and 20° inland, covering the Western Sahara and part of southern Spain. Finally, for the Benguela Current near ODP Site 1084, wetlands are added south of 10°S

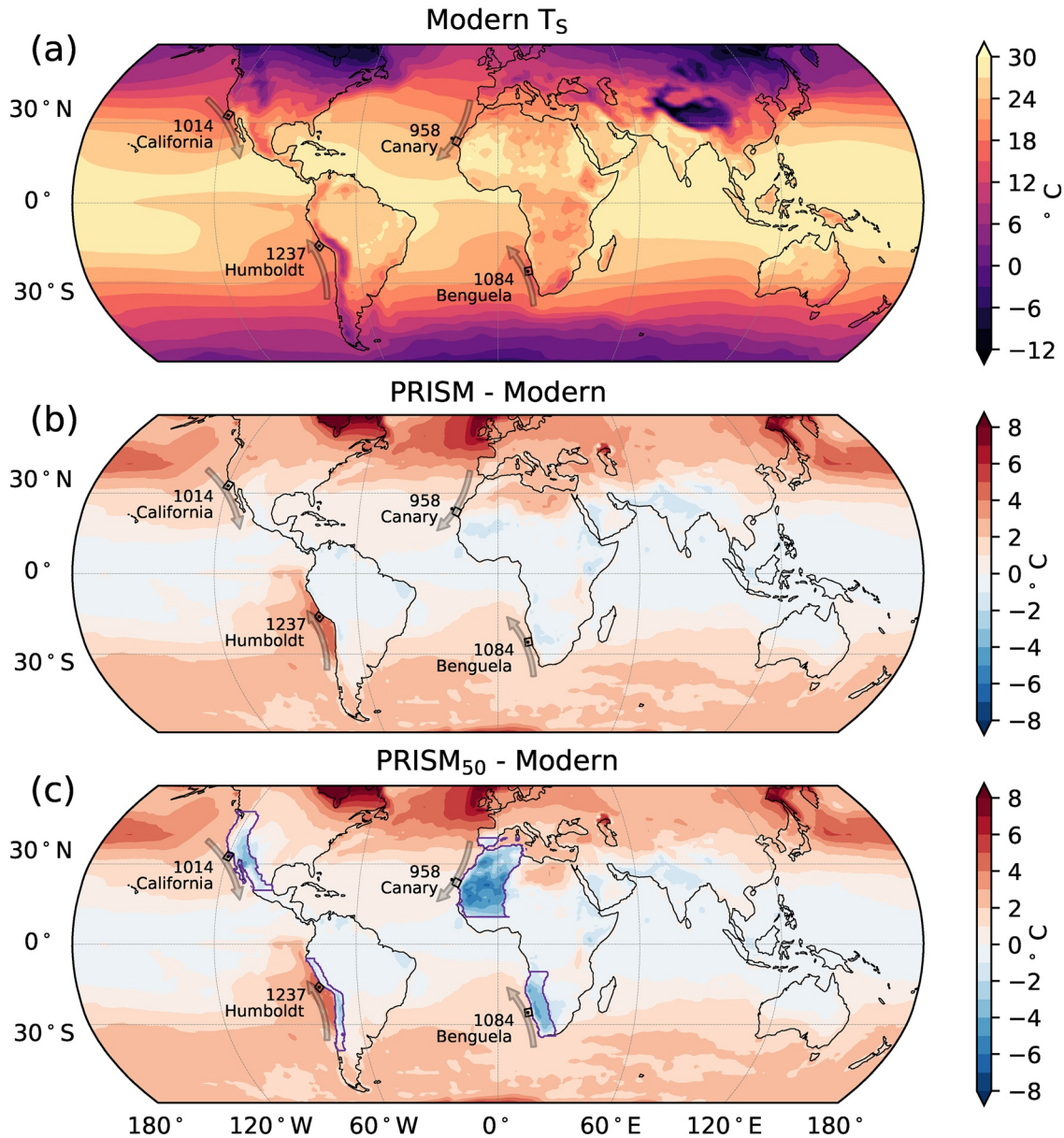

Figure 1. (a) Global surface temperatures (contours) for Modern. (b) Difference between PRISM and Modern. (c) Difference between $PRISM_{50}$ and Modern. Black dots and boxes indicate the Ocean Drilling Program sediment core sites and their corresponding 300 by 300 km coastal boxes. Locations of eastern boundary currents are labeled in all panels. Purple contours in panel (c) indicate the coastal regions where wetlands are prescribed.

to the southern tip of Africa at around 35°S, and extending 8° inland. Wetlands of varying grid-cell percentages are added to the Pliocene simulations using PRISM SST and Pliocene CO_2 but with modern vegetation.

The locations of the prescribed wetlands are visualized in contours in Figure 1c. The latitudinal ranges are chosen to surround each ODP site while the longitudinal ranges are chosen to largely enclose the arid regions near the western continental boundaries. Although the spatial patterns we chose are to some degree subjective, we found that widening the longitudinal extent of the wetland has minimal effects on upwelling favorable winds. In general, as long as the wetland encloses the deserts near the coast, the upwelling winds at the ODP sites are insensitive to variations in the zonal or meridional extent. Additionally, we remark that wetland percentage can be best understood as a variable used to tune surface moisture fluxes to match the characteristics of wetter land types, and that the values do not strictly correspond to the presence of actual

wetlands. Grid-cell percentages of 25%, 50%, and 100% are used in the $PRISM_{25}$, $PRISM_{50}$, and $PRISM_{100}$ experiments respectively.

2.3. Upwelling Indices

Upwelling indices used in this study follow the definitions used by previous studies (Arnold & Tziperman, 2016; Li et al., 2019). We distinguish between coastal and offshore upwelling. Coastal upwelling is caused by AWS parallel to shore, which causes offshore transport and cold upwelling from below. Offshore upwelling, on the other hand, is caused by the curl of surface wind stress leading to surface divergence. Coastal and offshore upwelling (Bakun & Nelson, 1991; Marshall & Plumb, 2008) are defined by the equations

$$M_{\text{coast}} = \tau_{\text{as}}/f \tag{1}$$

$$M_{\text{off}} = (\nabla \times \vec{\tau})/f \tag{2}$$

where τ_{as} is the alongshore component of $\vec{\tau}$, the wind stress vector. From the coastal point nearest to each of the four relevant ODP sites in the California, Canary, Humboldt, and Benguela Currents, a box is defined extending 150 km alongshore in each direction and 300 km out to sea. The coastal and offshore upwelling indices are defined as averages of the above equations over the ocean cells within the 300 km by 300 km box, and the offshore index is multiplied by 300 km to bring it to the same units as the coastal index.

2.4. Strong Upwelling Events

It has been found that in order to bring enough cold water to the surface to lead to observable SST differences, upwelling-favorable wind events should meet thresholds for duration (Botsford et al., 2006; Dugdale et al., 2006) and strength (Largier et al., 2006; Wilkerson et al., 2006). Following the definition from a previous study (Li et al., 2019), we define strong upwelling wind-events as events with an alongshore wind speed of 5 m/s persisting for at least 3 days. We use daily averaged winds and surface stresses to identify upwelling events and compute their deduced cumulative upwelling.

2.5. Track Analysis

To analyze storm track shifts and to help explain changes to coastal upwelling variability, we perform feature tracking of atmospheric anticyclones using the TRACK program (Hodges, 1994). For input, we use 6-h instantaneous sea level pressure (SLP) data. At every timestep a spectral filter removes the large scale background by decomposing the SLP into spherical harmonics and setting the total wave numbers less than six to zero (Hodges, 1996). Filtered trajectories of anticyclone centers are used, corresponding to the anticyclone tracks that persist for at least 1 day and have a track length exceeding 1000 km. Track densities are presented in units of $km^{-2}year^{-1}$ and are computed by normalizing the number of cyclones tracks per year in a grid cell by the grid cell area. This produces a result that is independent of model resolution.

3. Results

Modern annual-mean surface temperatures are shown in Figure 1a, and differences between PRISM and Modern are shown by the difference map in Figure 1b. Over the ocean (where SST is prescribed), surface warming is prominent at high latitudes, although PRISM generally does not include marked warming over the midlatitude upwelling sites. Some localized Pliocene warmth is found near the Humboldt upwelling site, as well as in the northeast Atlantic ocean and in the midlatitude Pacific around 40°N. Over land (where surface temperatures are instead prognostic), differences between PRISM and Modern are small near the subtropical upwelling sites (Figure 1b). In the $PRISM_{50}$ experiment, however, the prescribed wetter land conditions along the coasts near the upwelling sites result in an increase of latent heat flux and reduction of sensible heat flux to the atmosphere, which leads to surface cooling in these regions (Figure 1c). Diagnostics for $PRISM_{25}$ and $PRISM_{100}$ are shown in Figure S2 in Supporting Information S1. As we will show shortly,

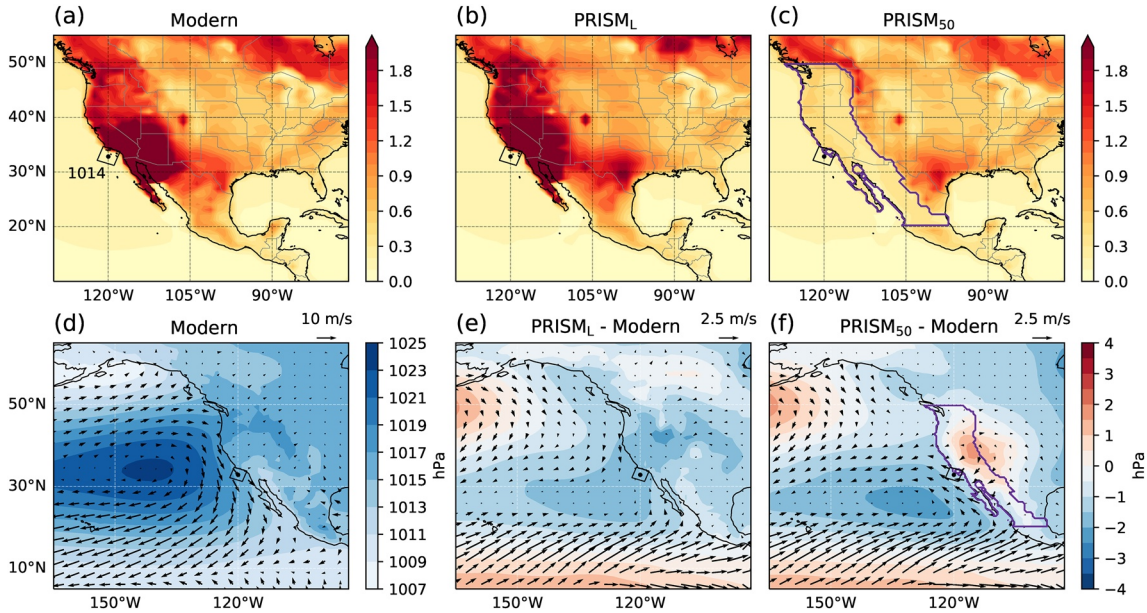

Figure 2. (a) Bowen ratio (contours) for Modern over North America. (b), (c) As in (a), but for PRISM$_L$ and PRISM$_{50}$. (d) Climatology SLP (hPa, contours) and surface winds (arrows) for Modern. (e) As in (d), but for differences between PRISM$_L$ and Modern. (f), as in (d), but for differences between PRISM$_{50}$ and Modern. The purple contours in (c) and (f) indicate the coastal regions where wetlands are prescribed.

this cooling leads to increased sea level pressure (SLP) over the regions of prescribed wetland, and therefore strongly weakens upwelling-favorable alongshore winds near the ODP sites.

We begin by analyzing changes around the California Current near ODP Site 1014. Figure 2a shows the Bowen ratio, the ratio between sensible and evaporative surface heat fluxes (Bowen, 1926), in the Modern experiment over North America. The Bowen ratio is commonly used for characterizing land types, and depends on surface moisture, temperature, and other factors. The modern American Southwest is characterized by broad regions of Bowen ratio above 2.0, consistent with observations from arid and semi-arid landscapes similar to those in this region (Laymon & Quattrochi, 2004; Malek et al., 1990; Sturman & McGowan, 2009). As indicated by high Bowen ratios, this region becomes only slightly less arid with PRISM SST and wetter-climate vegetation types (PRISM$_L$ experiment, Figure 2b).

Having found that the introduction of elevated CO_2 concentrations and Pliocene boundary conditions (e.g., SST, vegetation) alone do not simulate significantly moister subtropical continents, we raise subtropical land wetness by prescribing varying grid-cell percentages of wetland near the ODP sites. Figure 2c shows that when 50% wetlands are prescribed over the subtropical coast of North America, Bowen ratios in the desert regions of the Southwest US decrease to 0.3–0.4, similar to present-day eastern Colorado, and consistent with the characteristics of grasslands and forests (Stull, 2012; Twine et al., 2000). As the specified wetlands may be more consistent with a forested landscape rather than PRISM vegetation cover, we tested the effect of prescribing forested vegetation cover without specifying wetlands. We found that this does not directly change surface moisture availability and hence has minimal effects on the Bowen ratio and upwelling-favorable winds (not shown). Differences in Bowen ratios near the other upwelling sites, shown in Figures 3–5, show similar changes, consistent with the proxy record. We estimate that in these regions, prescribing 25%–50% fractional wetlands may be reasonable to bring surface fluxes into closer agreement with inferred Pliocene vegetation and land types, and we focus on experiment PRISM$_{50}$, as 50% is approximately the highest wetland percentage that is justifiable in this model configuration. Diagnostics for PRISM$_{25}$ and PRISM$_{100}$ are included in Figure S3 in Supporting Information S1.

Figure 2d shows the climatological annual-averaged SLP and surface wind field in the Modern experiment, including the North Pacific High and the associated mean upwelling winds to its east. Differences between PRISM$_L$ and Modern are shown in Figure 2e, indicating decreased SLP over the Pacific near 25°N and 130°W (shading), consistent with a large scale weakening of the North Pacific High caused by a reduced

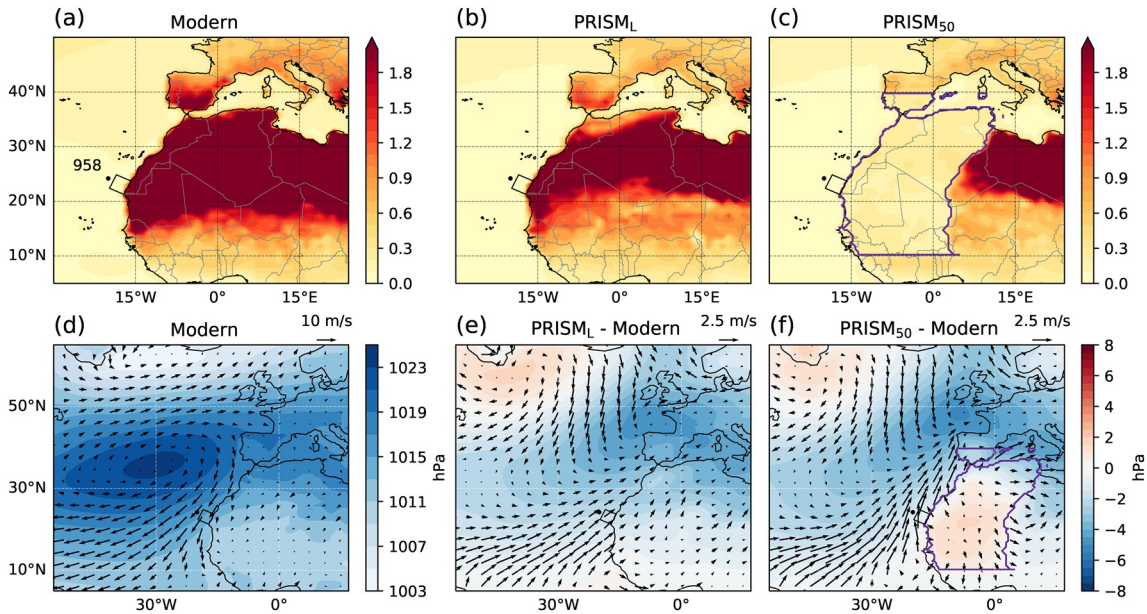

Figure 3. As in Figure 2, but for the Canary Current.

large-scale meridional temperature gradient. With the addition of wetlands (experiment PRISM$_{50}$), surface cooling leads to increased SLP near the upwelling sites over the region where wetlands are applied (Figure 2f); the combination of the weakened North Pacific High and increased SLP over land reduces the land-sea pressure gradient, resulting in a weakening of the geostrophically balanced alongshore winds near ODP Site 1014 (black dot).

Wetter boundary conditions lead to similar changes at ODP Site 958 near the Canary Current, with increases in SLP over land leading to weaker mean upwelling winds (Figure 3). At ODP Site 1237 off the coast of Peru, no strong changes occur due to the addition of wetlands (Figure 4). This site is also associated with the smallest inferred cooling since the Pliocene, consistent with the negligible changes we found. The Benguela

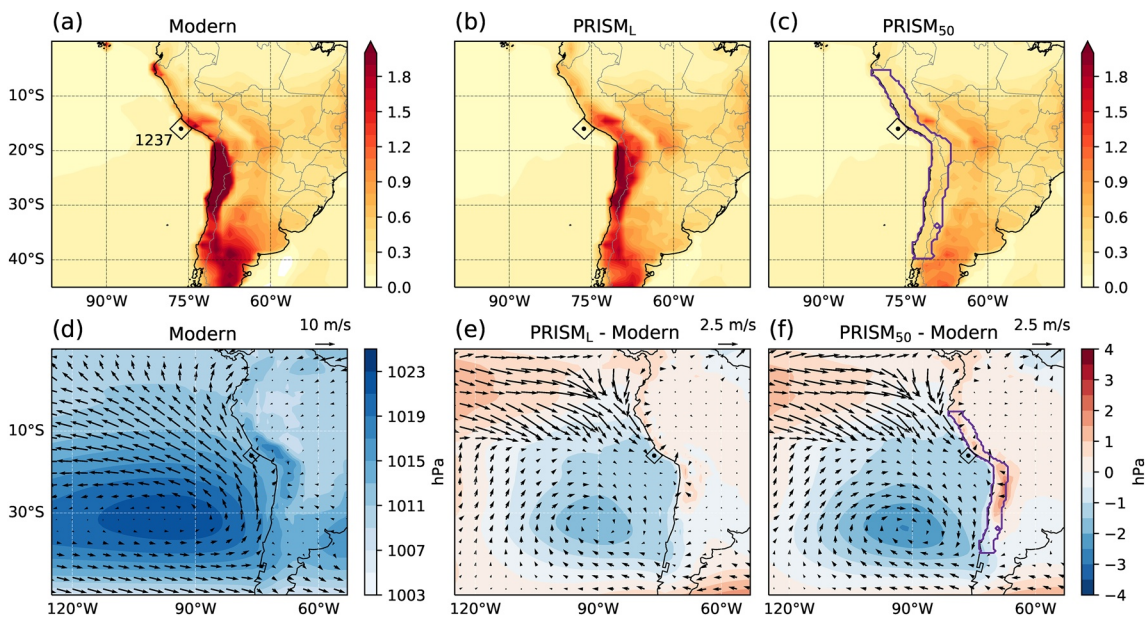

Figure 4. As in Figure 2, but for the Humboldt Current.

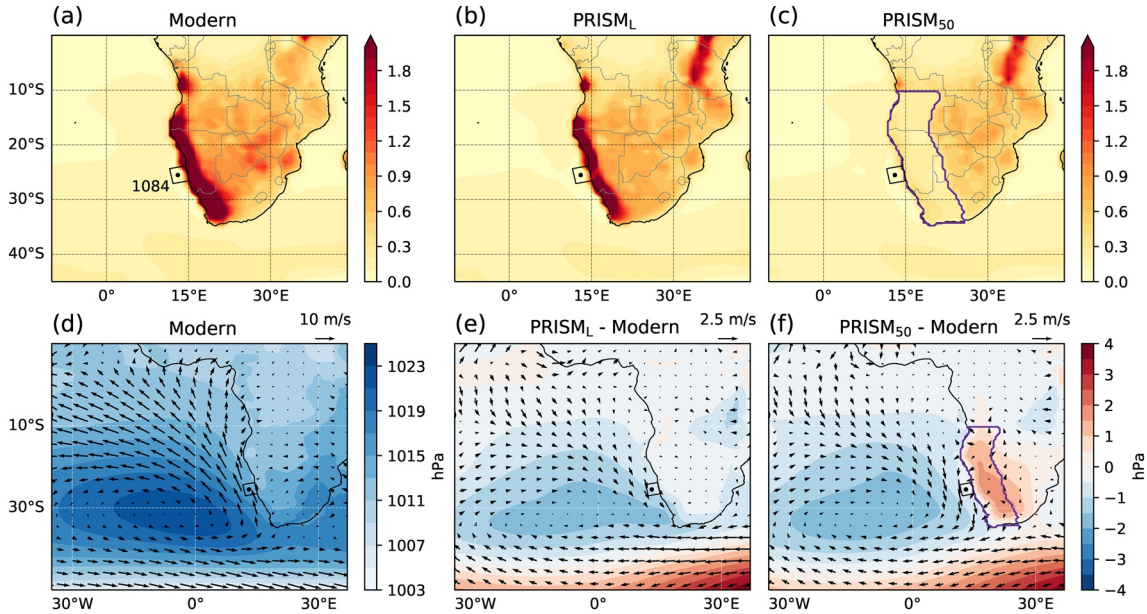

Figure 5. As in Figure 2, but for the Benguela Current.

Current at ODP Site 1084, consistent with the California and Canary Currents, shows pressure increases over land and weakening of the mean upwelling winds (Figure 5). A summary of annual mean coastal and offshore upwelling is shown in Figures 6a–6d, indicating considerable decreases to mean coastal and offshore upwelling indices with the addition of wetland.

Having found significant changes to the time-mean upwelling at three of the four upwelling sites, we now focus our attention on the statistics of transient coastal upwelling-wind events. Because sustained strong winds have a much greater effect on upwelling than average background winds, we calculated probability density functions (PDFs) of alongshore wind stresses (Figures 6e–6h). For the California, Canary, and Benguela Currents, the mean decreases and the PDF becomes skewed toward weak events when wetlands are added, corresponding to many fewer days associated with strong coastal upwelling-favorable wind events. We will see shortly that this dramatically decreases the deduced upwelling volume flux, and according to ocean model experiments, is expected to lead to a large surface warming consistent with the proxy observations (Miller & Tziperman, 2017).

To explain the change to the coastal upwelling-favorable wind-stress events, consider Figure 6i, which shows the PDFs of alongshore surface wind speeds near the California site. The distribution shape changes only slightly with the addition of wetland. The PDF shapes of wind speeds with and without wetlands over adjacent continents are also similar, but the mean is smaller for those with wetlands than without them (Figures 6i–6l). The dark green curve (Modern$_{shift}$) in Figures 6i–6l shows the PDF of the Modern alongshore wind constructed after shifting every daily index by the difference in daily climatology between PRISM$_{50}$ and Modern. The fact that the PDF of the shifted Modern winds (dark green) very closely resembles the PRISM$_{50}$ PDF (light green) indicates that the addition of wetland changes the mean alongshore wind speed but has very little effect on its variance and skew. The large changes to the distribution shape of the California site coastal upwelling-favorable wind stress seen in Figure 6e can therefore be attributed to the nonlinear dependence of wind stress on wind speed.

We also find latitudinal differences in storm tracks between Modern and Pliocene configurations (Figure 7b), similar to a previous study (Li et al., 2019). On the other hand, the changes to the storm tracks from the addition of wetlands are minimal, so this shift is not a significant factor in reducing upwelling-favorable winds (Figure 7c).

We next consider the dependence of integrated annual coastal upwelling due to strong upwelling events on the degree to which onshore regions are converted into wetlands (Figure 8). The reduction in cumulative

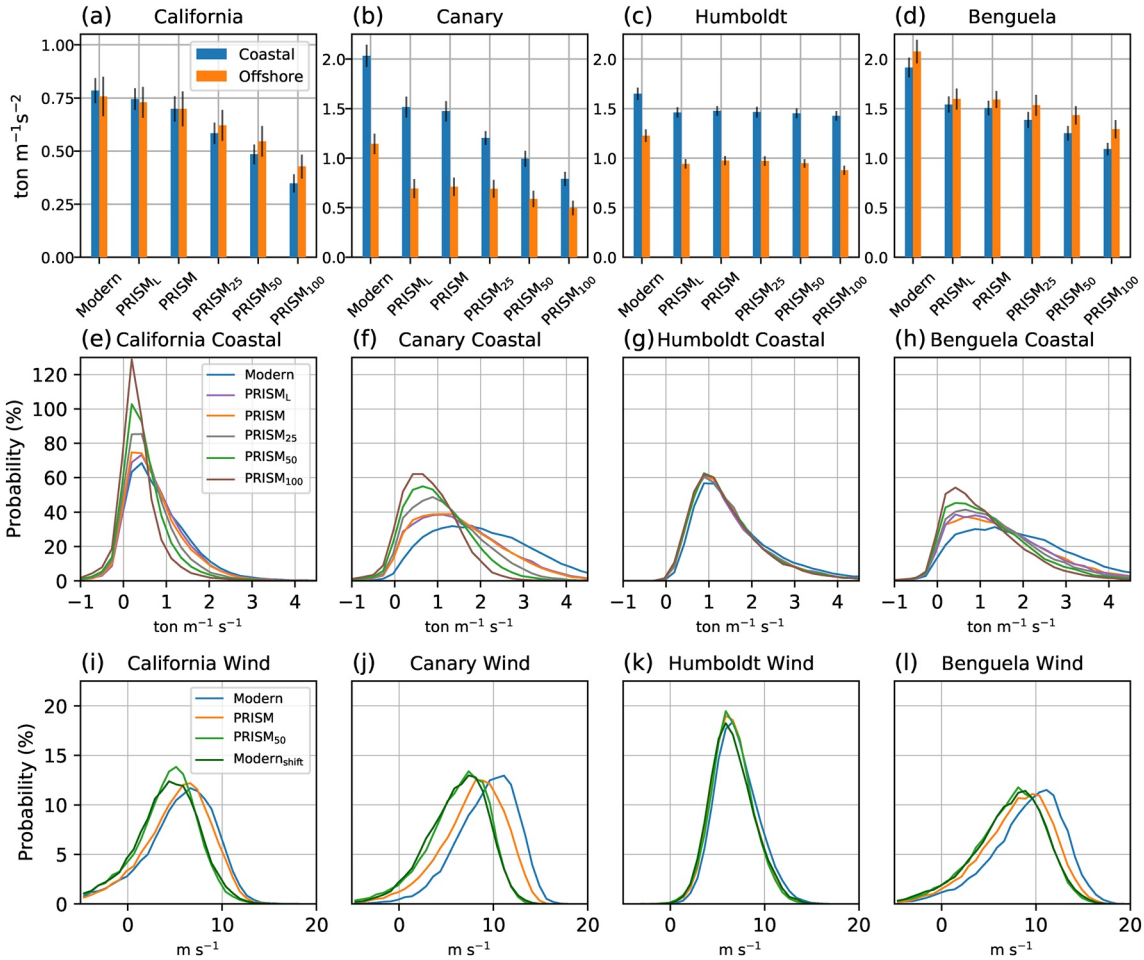

Figure 6. (a)–(d) Annual-mean coastal and offshore upwelling indices at the California, Canary, Humboldt, and Benguela Currents. (e)–(h) Probability density functions (PDFs) of daily averaged coastal upwelling indices over the final 75 years of the simulations constructed for the California, Canary, Humboldt, and Benguela Currents. (i)–(l) PDFs constructed for the daily alongshore wind speed for the four upwelling sites, with the inclusion of $\text{Modern}_{\text{shift}}$. $\text{Modern}_{\text{shift}}$ is constructed by calculating the PDF of Modern after shifting the daily alongshore wind by the difference in daily climatology between PRISM_{50} and Modern. Error bars in (a)–(d) represent one standard deviation of the annual upwelling index over the simulation period ($n = 75$).

upwelling flux varies roughly linearly with the grid-cell percentage of wetlands that is prescribed. The decrease in upwelling due to the wetlands is particularly strong for the California site, where the Pliocene temperature difference was especially large, and where the decrease in upwelling wind is mostly due to addition of wetlands rather than from the change from Modern SST to the Pliocene PRISM SST. The Canary and Benguela sites show moderate decreases in upwelling when switching from Modern conditions to PRISM, and roughly comparable further decreases with the addition of wetlands. Again, the Humboldt Current is insensitive to the presence of wetlands, consistent with the Pliocene-present SST difference of only +2.9°C, close to the global mean temperature difference relative to present-day, and thus not requiring local mechanisms such as wind changes to explain. The cumulative coastal and offshore upwelling indices for each month are shown in Figure S4 in Supporting Information S1.

Overall, the addition of 50% wetland near the coast led to reductions in deduced upwelling event flux to the order of 40%–50% for several of the upwelling sites. When wetlands are added near the various ODP sites, wind stress curl also weakens, leading to decreases in the offshore upwelling measure as well. Figure 9 shows changes in surface wind stress (arrows) and offshore upwelling (shading) for the four upwelling regions under experiments PRISM and PRISM_{50}. Diagnostics for PRISM_{25} and PRISM_{100} are shown in Figure S5 in Supporting Information S1. High resolution ocean modeling of the effect of changes in Pliocene surface winds on SSTs in an idealized configuration (Miller & Tziperman, 2017) suggests that a 50% reduction

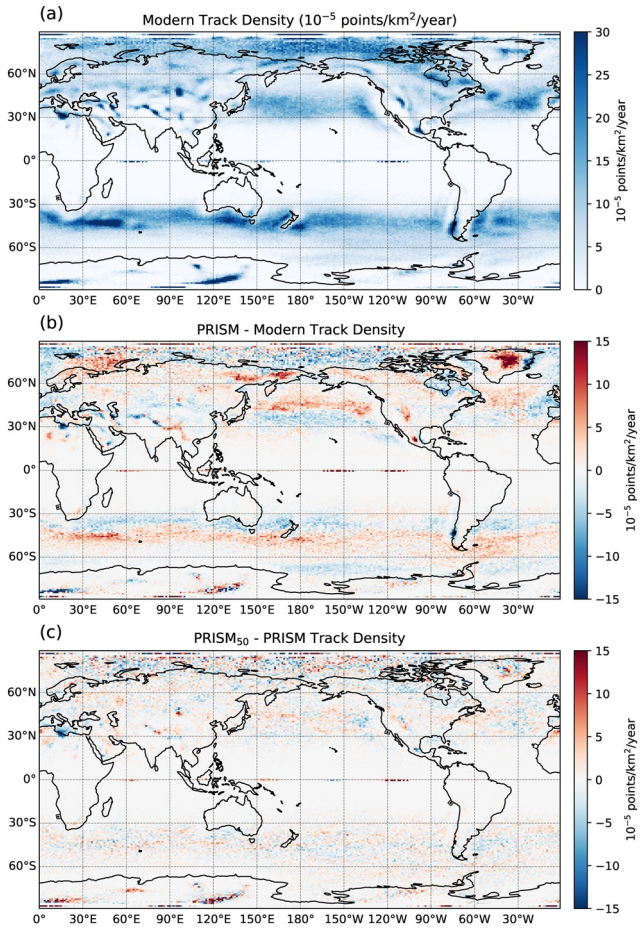

Figure 7. (a) Anticyclone track density for the final 75 years of the Modern simulation. (b) Difference between PRISM and Modern. (c) Difference between $PRISM_{50}$ and PRISM.

in mean wind stress, plus the global mean Pliocene warming (taken as 3°C) may lead to up to 7.1°C SST warming near the coast and 5.5°C at the offshore proxy sites. The differences in upwelling winds we found can therefore help rationalize much of the SST differences inferred near the California (+8.8°C), Canary (+4.1°C), and Benguela (+9.3°C) currents (Dekens et al., 2007; Herbert & Schuffert, 1998; Marlow et al., 2000).

4. Discussion and Conclusions

Coupled General Circulation Models (GCMs) generally show the largest data-model mismatches over midlatitude coastal upwelling regions, particularly near the Benguela current (Dowsett et al., 2013; Fedorov et al., 2013; Haywood et al., 2020; McClymont et al., 2020). A recent data set now shows much smaller SST differences between mid-Pliocene and present-day at the California and Canary currents (Foley & Dowsett, 2019), although their target was the mid-Piacenzian rather than the earlier period which we study. ODP Sites 1012 (Brierley et al., 2009), 1014 (Dekens et al., 2007), and 1021 (LaRiviere et al., 2012), which showed early-Pliocene SST warmth, were absent from Foley and Dowsett (2019) and the model-data intercomparison of Haywood et al. (2020). Future studies should investigate whether the inferences of warm upwelling site temperatures during the early Pliocene can now be reproduced in coupled climate models. Additionally, Pliocene upwelling wind reductions in atmospheric GCMs run with prescribed Pliocene sea surface temperature boundary conditions contribute to, but fall short of accounting for the dramatic temperature differences at some of those upwelling sites (Arnold & Tziperman, 2016; Li et al., 2019).

We find that adding fractional wetlands over the coastal subtropics near midlatitude upwelling sites, consistent with inferred Pliocene conditions (Herbert et al., 2016; Thompson & Fleming, 1996), leads to a decrease in both mean upwelling-favorable winds and transient upwelling wind events. The wetlands affect land-sea pressure gradients near the coastal areas, which in turn weaken the geostrophically balanced alongshore winds on the eastern boundaries of the Pacific and Atlantic basins. These differences in mean wind speeds near coastal upwelling sites lead to nonlinearly related differences in along-coast wind stress, helping explain warm Pliocene coastal SSTs inferred from proxy based SST reconstructions. Although it is difficult to precisely determine the amount of surface water and soil moisture availability during the Pliocene based on proxy evidence, on the basis of surface fluxes, somewhere between 25%–50% fractional wetland in the prescribed regions appears justifiable in the model configuration we used. While observed Pliocene conditions do not directly support the prescribed wetlands, the idealized experiment of 50% wetland prescribed in relatively restricted coastal areas (experiment $PRISM_{50}$) leads to reductions in upwelling flux of the order of 40%–50% at the three out of four upwelling sites. Such reductions were shown by high-resolution regional idealized Pliocene ocean simulations to potentially lead to +7.1°C warming near the coast (Miller & Tziperman, 2017), which explains a significant part of the large off-California warming.

A feature of the experiments presented here is that is arguably not self-consistent, is the fact that parts of the regions where wetlands are prescribed are characterized by negative values of precipitation minus evaporation ($P - E$) that monotonically decrease with increasing grid-cell wetland percentage (Figure S6 in Supporting Information S1). This may be a result of the increased subsidence over the prescribed wetlands (not shown). This suggests that strictly speaking, the prescribed wetlands simulated here cannot be sustained by the model's large-scale atmospheric circulation. This highlights the challenges that climate models face in simulating accurately simulating the Pliocene hydrological cycle, and may also be a result of the prescribed large-scale SST patterns used as boundary conditions. Given the idealized nature of our

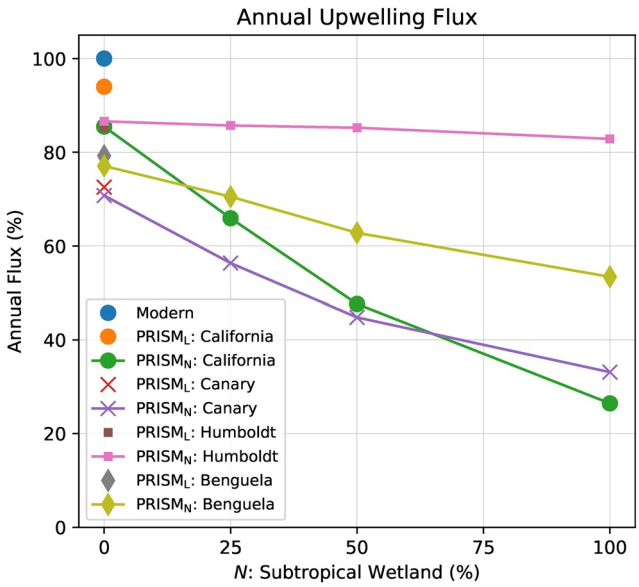

Figure 8. Deduced cumulative annual coastal flux from strong upwelling days at the four Ocean Drilling Program upwelling sites. The annual upwelling flux is calculated by integrating the coastal upwelling index over all days flagged as strong upwelling events. The cumulative flux as a percentage of Modern is plotted as a function of the prescribed wetland percentage.

experiments, explaining the source of the excess precipitation is outside of the scope of this study. Reduced meridional SST gradients (Burls & Fedorov, 2017) or the possible existence of a "permanent El Niño" (Molnar & Cane, 2002, 2007) may have contributed to sustaining wetter conditions that were inferred over land.

We note that proxy reconstructions of SSTs are coupled to biological productivity, and hence may be biased towards times during which this productivity is especially large. If the productivity is strongly influenced by the availability of nutrients brought by upwelling from the deep ocean, then one expects the proxy SST to reflect the SSTs during times of upwelling events. In that case, our integrated upwelling flux index, which sums over these upwelling events, may be a close reflection of the same quantity represented by the proxy SST record.

We remark that there is likely some diversity in the mechanisms leading to Pliocene warmth at the different ODP sites. We find little change in upwelling-favorable winds near the Humboldt Current (ODP Site 1237), consistent with the relatively small inferred Pliocene SST of +2.9°C (Dekens et al., 2007). This difference may be accounted for solely by the global-mean Pliocene surface warming. The lack of wind response near this site may be due to a few different factors. ODP Site 1237 is located relatively equatorward, at 16°S, north of the Atacama Desert in northern Chile as well as north of the South Pacific High. Along-coast winds near this site are therefore less sensitive to surface pressures over the Atacama Desert region south of the site, and therefore to soil moisture there. The Atacama Desert is very narrow, so the narrow strip of wetlands we prescribe also does not significantly alter the local atmospheric sea level pressure field and circulation. Furthermore, the upwelling-favorable winds in that area are forced by the Andes topography which redirects the winds equatorward along the Chilean coast (Rodwell & Hoskins, 2001; Takahashi & Battisti, 2007), rather than relying only on the zonal land-sea contrast. We also note that a relatively small temperature difference of +4.1°C (Herbert & Schuffert, 1998) from Pliocene to present was found at ODP Site 958 near the Canary current. This site, however, is farther offshore than ODP Sites 1014 and 1084 near the California and Benguela currents. A site closer to the coast of West Africa would likely reflect a similarly large SST difference between Pliocene and present time.

Finally, we recognize that our atmospheric-only simulations are run with fixed SSTs and hence do not capture possible atmosphere-ocean feedbacks. For example, warmer coastal SSTs due to upwelling weakening could reduce the land-sea temperature gradient and further reduce upwelling winds, strengthening the wind changes found here. However, the narrowness of the upwelling zones (~10–50 km) relative to the large scales of atmospheric motions (1000s of km), suggests such a feedback on the atmospheric circulation may be weak, which justifies our use of an atmosphere-only model. Another positive feedback may result from a further moistening of the subtropical land due to the reduced upwelling and higher SSTs along the coast, leading to increased atmospheric moisture transport into the continent. Given the difficulty of reconstructing soil moisture over the continental areas near coastal upwelling sites, we resorted to specifying a range of idealized wetter conditions, making our experiments somewhat speculative yet seemingly plausible. Nonetheless, our results show that reduced upwelling winds resulting from increased subtropical land wetness may play an important role in explaining the dramatically warmer Pliocene SSTs inferred at major coastal upwelling sites.

Appendix A: Evidence of Wetter Pliocene Subtropics

Numerous studies have presented qualitative evidence suggesting that subtropical continents received more rainfall during the Pliocene than today. Virtually none offers quantitative estimates of differences in rainfall. Moreover, most sample points, not areas, and most report evidence for instants in geological time,

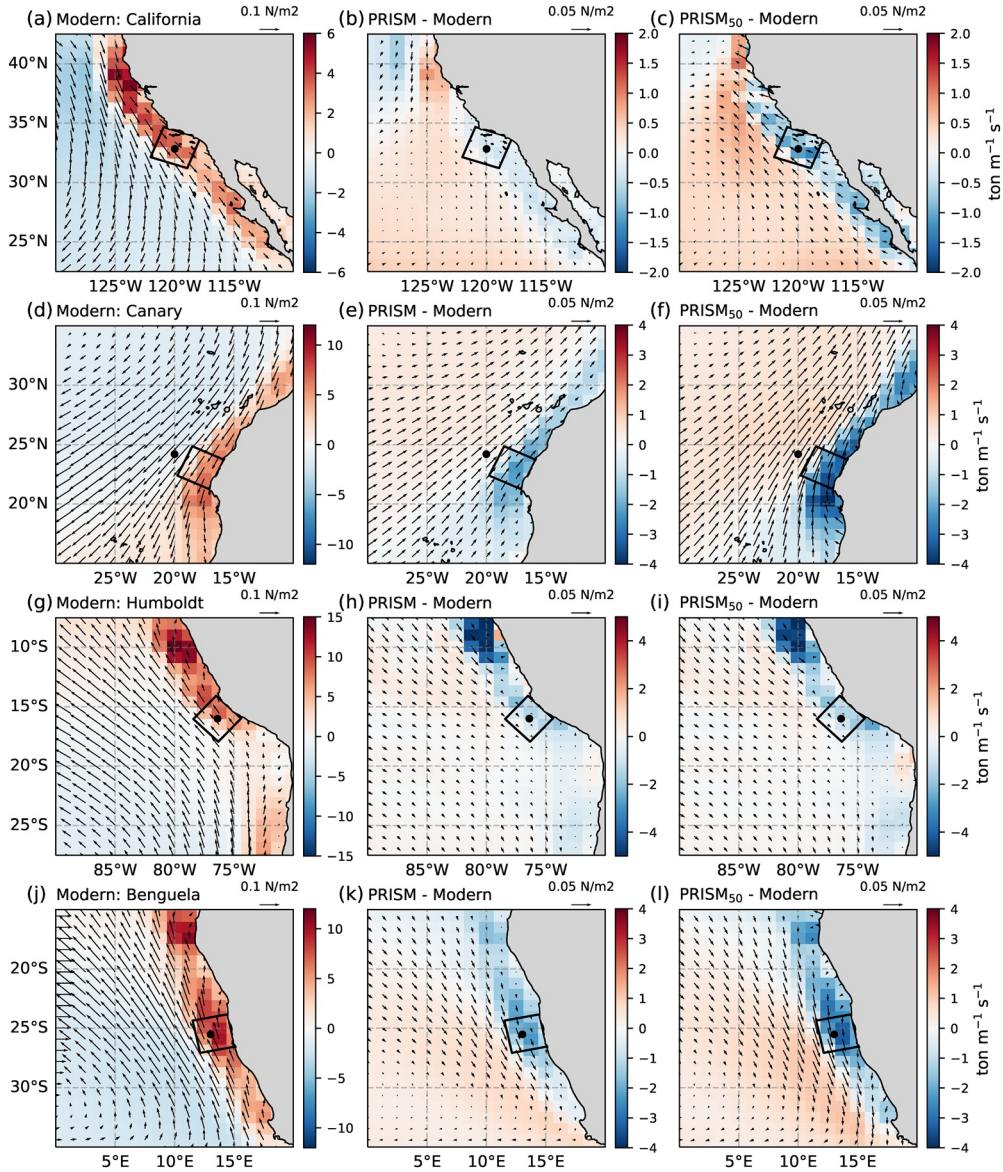

Figure 9. Offshore upwelling (shading) and surface wind stress (arrows) for Modern experiment (left column) and differences between PRISM and Modern (middle column) and between $PRISM_{50}$ and Modern (right column). Analysis done at the California (a)–(c), Canary (d)–(f), Humboldt (g)–(h), and Benguela (j)–(l) upwelling sites.

rather than continuous time series spanning millions of years. In the following paragraphs, we review such data, and in Table A1 we summarize these data.

Table A1
Summary of Evidence of Wetter Subtropical Continents During the Pliocene

Latitude	Longitude	Age (Ma)	Climate	Reference
Western USA				
45.4	−122.6	2.9	Drier (1000 mm)	Wolfe (1990)
42.9	−115.8	3.5–2.5	Wetter	Thompson (1996)
42.8	−115.3	3.7–3.3	Wetter	Forester (1991)
42.7	−114.9	3.5–3	Wetter	Leopold and Wright (1985)

Table A1
Continued

Latitude	Longitude	Age (Ma)	Climate	Reference
42.7	−114.9	3.7–3.3	Wetter	Forester (1991)
42.7	−114.9	3.7–3.3	Wetter	G. R. Smith (1987); G. R. Smith and Patterson (1994)
42.0	−121.5	3.0–2.5	Wetter	Adam et al. (1989); Adam et al. (1990); Thompson (1991)
41.6	−111.8	>2.5[a]	Wetter (100 mm)	Brown (1949); Thompson (1991); Wolfe (1990)
41.5	−120.5	4.8	No difference	Forester (1991)
41.2	−112.6	5–2.5	Wetter	Davis and Moutoux (1998)
41.1	−112.8	5–0.6	Wetter	Kowalewska and Cohen (1998)
40.8	−112.5	5–1.6	Wetter	Kowalewska and Cohen (1998)
38.2	−118.0	>2.5[a]	Wetter	Reheis et al. (2002)
38.0	−118.8	4.–3.	Wetter	Reheis et al. (2002)
37.9	−118.0	3.4–2.8	Wetter	Reheis et al. (2002)
37.7	−117.6	4.0–2.0	Wetter	Reheis et al. (2002)
37.4	−106.0	3.5–0.4	Wetter	Machette et al. (2013)
37.1	−103.5	3.7–2.6	Wetter	Hager (1974); Thompson (1991)
36.5	−116.2	3.4–3.2	Wetter	Hay et al. (1986)
36.5	−114.1	4.8	Wetter	Spencer et al. (2013)
36.0	−117.0	3.5–3.3	Wetter	Knott et al. (2008); Knott et al. (2018)
35.7	−117.5	3.6–3.2	Wetter	G. I. Smith (1984)
35.3	−106.3	4.5–2.5	Wetter	Connell et al. (2013); Bartolino and Cole (2002)
35.1	−106.6	4.7–0.8	Wetter	Connell et al. (2013); Bartolino and Cole (2002)
35.	−112.	4.5–4.0	Wetter	Forester (1991)
34.9	−114.2	4.8	Wetter	Spencer et al. (2013)
34.2	−114.1	4.8	Wetter	Spencer et al. (2013)
33.7	−114.4	4.8	Wetter	Spencer et al. (2013)
33.0	−116.1	3.8–2.6	Wetter	Remeika et al. (1988)
32.0	−101.5	3.2	Wetter	Thompson (1991)
31.9	−106.4	4.9–1.8[b]	Wetter	Collins and Raney (1994); Stuart and Willingham (1984)
31.8	−110.3	3.4–2.8	Wetter	G. A. Smith (1994); G. A. Smith et al. (1993)
20.3	−98.7	4.6–2.5	Wetter	Velasco-de León et al. (2010)
20.2	−102.5	7.0–2.5	Wetter	Israde-Alcántara et al. (2010)
19.9	−101.0	6.0–3.0	Wetter	Israde-Alcántara et al. (2010)
Western South America				
−14.7	−71.3	4.8	Wetter	Martínez et al. (2020)
−18.5	−69.5	6.4–3.7	Wetter	Gaupp et al. (1999)
−19. to −21.6	−70. to −69.	>3.5	Wetter	Allmendinger et al. (2005)
−19.75 to −23.	−69.	>3–4	Wetter	Hartley and Chong (2002)
−21.	−70.	>3–4[c]	Wetter	Chong Díaz et al. (1999)
−21.5	−69.	>6.4	Wetter	Sáez et al. (1999)
−23.	−70.5	>3–4	Wetter	Arancibia et al. (2006)
−26.35	−69.9	>2.4; <5–6	Wetter	Amundson et al. (2012)

Table A1
Continued

Latitude	Longitude	Age (Ma)	Climate	Reference
−26.5	−65.8	>3.	Wetter[d]	Sobel and Strecker (2003)
−26.7	−66.0	>3.	Wetter[d]	Kleinert and Strecker (2001)
West Africa and western Mediterranean				
26.8	−15.2[e]	>3.2	Less dust	Tiedemann et al. (1989)
21.3	−20.9[e]	>2.5	Less dust	Tiedemann et al. (1989)
20.7	−18.6[e]	3.5–2.6	Wetter	Leroy and Dupont (1994); Leroy and Dupont (1997)
20.7	−18.6[e]	>3.5	Less dust	Tiedemann et al. (1989)
18.1	−21.0[e]	>4.	Less dust	Tiedemann et al. (1989)
17.	18.	5.3	Wetter	Otero et al. (2009a); Otero et al. (2011)
16.5	17.6	5.–4.	Wetter	Zazzo et al. (2000)
16.2	17.5	7.–6.	Wetter	Louchart et al. (2004)
16.2	17.5	3.6.–3.0	Wetter	Vignaud et al. (2002)
16.2	17.5	3.6.–3.0	Wetter	Otero et al. (2010); Otero et al. (2011)
16.0	18.9	7.–3.5	Wetter	Otero et al. (2009a); Otero et al. (2009b)
16.0	18.9	3.5–3.0	Wetter	Brunet et al. (1995)
13.5	14.7	6.3–2.5	Wetter	Novello et al. (2015)
13.5	14.7	6.5–2.4	Wetter	Moussa et al. (2016)
10.0	−19.2[e]	>4.	Less dust	Tiedemann et al. (1989)
9.5	−19.4[e]	>4.	Less dust	Tiedemann et al. (1989)
17.	17.	>4.6	Wetter	Griffin (2002); Griffin (2006) (Lake Chad)
14.	9.	>4.6	Wetter	Griffin (2002); Griffin (2006) (Lake Chad)
10.	18.	>4.6	Wetter	Griffin (2002); Griffin (2006) (Lake Chad)
Southwest Africa, Namibia, Angola, and western South Africa				
−21.1	11.8	3.4–2.7	Wetter	Dupont (2006); Dupont et al. (2005)
−22.	14.	>2.5	Wetter	Namaqualand[f]
−24.2	29.2	3.33–2.58	Wetter	Makapansgat[g]
−25.3	15.6	>3.5	Wetter	Segalen et al. (2002)
−26.0	27.7	3.3–2.58	Wetter	Bamford (1999)
−28.5	16.5	>3.5	Wetter	Segalen et al. (2002)
−29.4	14.0	>4.5	Wetter	Dupont et al. (2013)

[a]Mio-Pliocene; no numbers were given. [b]Within the Blancan North American Stage. [c]Late Pliocene; no numbers were given. [d]Aridification could be due to tectonic uplift of an orographic barrier. [e]These are Ocean Drilling Program sites and they refer to inferences of climate to the east of them. [f]Namaqualand (Cowling et al., 2005; Pickford & Senut, 1997; Pickford et al., 1999; Scott, 1995). [g]Makapansgat (Cadman & Rayner, 1989; Rayner et al., 1993; Sloggett, 2016) (Suggestions of a wetter climate).

This appendix includes many references cited by previous compilations (Burls & Fedorov, 2017; Pound et al., 2014; Salzmann et al., 2008), as well as others not cited by those studies. Pound et al. (2014) focused on the somewhat later period of the late Piacenzian (3.6–2.6 Ma) rather than the earlier period corresponding to the warm upwelling sites we are interested in. While in some cases the wetter conditions near the upwelling sites are marked at a single grid cell in their reconstruction, nearby grid points with no relevant data may have been wetter as well. Indeed Pound et al. (2014) mentioned that regions such as the Sahara may have been covered with river systems which were not represented in their reconstruction.

Pound et al. (2014) wrote: "Northern Africa was dominated by Lake Chad, which was considerably bigger than in modern times during the late Pliocene (Otero et al., 2010; Schuster et al., 2009)." We also used Schuster et al. (2009) and Otero et al. (2010). Pound et al. (2014) wrote few words about western North America.

"In North America there is a swarm of small to modest-sized lakes associated with the valleys of the Rocky Mountains (Figures 2b and 2c). The largest of these was Glenn's Ferry in Idaho, which has been reconstructed from sediments and the distribution of fossil fishes (G. R. Smith, 1981; Thompson, 1992)." We also used studies by Smith and Thompson and more.

Appendix A1: Western North America

Previous studies have synthesized evidence for Pliocene paleoclimate showing that most of western North America was wetter before than since ~2.5 Ma (Thompson, 1991; Thompson & Fleming, 1996), and updated syntheses have added some corroborating data (Ibarra et al., 2018; Molnar & Cane, 2002, 2007; Winnick et al., 2013). Although fossil leaf physiognomy from the Oak Grove Fork site in northern Oregon suggested that mean annual rainfall at ~2.9 Ma was 1000 mm less than today (Wolfe, 1990), for nearly all sites south and southeast of this one, wetter climates characterized Pliocene time, with 2.5 Ma approximating the time when aridity became most obvious. Three kinds of evidence suggest wetter Pliocene than present climates: the presence of lakes, paleobotanic evidence of different climates, and stable isotopes of carbonate sediment.

Lakes were widespread across western North America in Pliocene time (Ibarra et al., 2018). It has been inferred that in Miocene and Pliocene time "Lake Idaho," which sprawled across southern Idaho and left an abundance of lacustrine deposits and fish and other fossils (Forester, 1991; G. R. Smith, 1987), was as large as Lake Ontario today (G. R. Smith & Patterson, 1994). McClellan and Smith (2020) reported fish fossils similar to those in Lake Idaho in lacustrine deposits farther south and east reaching into northern Utah that suggest connections between lakes in these regions, including Cache Valley (Figure S1 in Supporting Information S1). Pliocene lacustrine deposits found in drill cores through the Pleistocene Lake Bonneville also demonstrate moist Pliocene conditions (Kowalewska & Cohen, 1998). Farther south, in western Nevada, sparse outcrops of lacustrine deposits with interbedded tephra suggest wide-spread lakes where later Pleistocene lakes were large (Reheis et al., 2002). Evidence points towards a large Pliocene lake in the Bonneville Basin of northern Utah (Thompson, 1991). In the Death Valley region of southeastern California, widespread lacustrine sediment attests to several lakes occupying what are now dry basins between 3.5 and 3.3 Ma (Knott et al., 2008, 2018). One study used marl and clay at the bottom of the Searles Lake basin to infer that a lake existed from 3.2 to 2.6 Ma, when the region became too arid to sustain a perennial lake (G. I. Smith, 1984); another described a large Pliocene-mid-Pleistocene lake in the San Luis Valley in Colorado (Machette et al., 2013). Concurrently, lacustrine sediment in Pliocene formations of the Santa Fe Group were deposited in basins of the Rio Grande rift (Brister & Gries, 1994; Connell et al., 2013; Galusha & Blick, 1971), and apparently also in the Hueco Bolson (Collins & Raney, 1994; Stuart & Willingham, 1984). They suggest a moist Pliocene that later gave way to a more arid Pleistocene climate (e.g., Bartolino & Cole, 2002). A series of four large lakes, one in excess of 10,000 km^2 in extent and the others together reaching nearly half that size seemed to occupy the region between Lake Mead and the Gulf of California at 4.8 Ma, though all three might not have been full at the same time and their durations seem unconstrained (e.g., Spencer et al., 2013). Farther south, in Mexico, vegetation and thicknesses of lacustrine deposits with diatoms suggest a wet phase between 5.3 and 3.8 Ma between ~20.3°N, 103.3°W and 19.8°N, 100.3°W (Israde-Alcántara et al., 2010). Moreover, both analyses of leaves and the presence of "gastropods, ostracods, small fishes, vertebrate remains, and some insects" in another lake basin at 20.3°N, 98.8°W were used to infer that that region was wetter in early Pliocene time than today (Velasco-de León et al. (2010)).

Among paleobotanical evidence of wet Pliocene climates, pollen assemblages deposited in the Lake Idaho region imply wetter Miocene and Pliocene (4–3 Ma) climates than present-day (Leopold & Wright, 1985; Thompson, 1996). Fossil leaf physiognomy suggests a drier Pliocene climate in one region and wetter in two others: annual rainfall 1000 mm less than today southeast of Mount Hood in Oregon, but 60 mm greater in the Cache Valley in northern Utah and 100 mm greater just north of San Francisco (Wolfe, 1990). Vegetation from the Lake Bonneville region suggests a steady cooling and aridification over Pliocene time (Davis & Moutoux, 1998). Similarly, fossil plants and animals from a region southeast of San Luis Valley in Colorado suggest a wet Pliocene environment there (Hager, 1974; Thompson, 1991). Furthermore, taxonomy of petrified wood in the Anza-Borrego region of southern California suggested a wetter climate between ~3.8 and 2.6 Ma than today's desert (Remeika et al., 1988). Although the shift from montane conifer forest to

pinyon-juniper-chaparral woodlands in the Great Basin has been attributed to a rising Sierra Nevada and its rain shadow (Minnich, 2007), aridification due to global climate change might be responsible for that shift. Another study reported vegetation in central Arizona at 4.5–4.0 Ma that suggested a wetter climate than present, but with little difference by 2.7–2.6 Ma (Forester, 1991).

From the chemistry of sediment, others have inferred wetter-than-present Pliocene conditions: in the basal sediment of Searles lake between 3.2 and 2.8 Ma (G. A. Smith et al., 1993), in deposits associated with springs deposited east of Death Valley in the Amargosa Basin between 3.2 Ma (their oldest material) and 2.5 Ma (Hay et al., 1986), and in sediment in southern Arizona (near 31.8°N; 110.3°W) from 3.4 to 2.8 Ma (G. A. Smith, 1994).

As the one exception, an ostracode assemblage at a site near the California-Oregon border implied little difference between early Pliocene and present-day climates (Forester, 1991).

Appendix A2: Western South America

Data from western South America is sparser and less definitive than that from western North America. Most evidence comes from northern Chile, which is famously hyperarid today. A range of dates have been given for when the hyperarid climate set in, and for different sites. Most evidence derives from evaporite deposits. It has been argued that a wetter Atacama "persisted until at least 5.6 Ma and if the age of the Pisagua tuff is reliable, until at least ca. 4 Ma" (Allmendinger et al., 2005). The $^{40}Ar/^{39}Ar$ isochron for the Pisagua tuff gives 3.49 ± 0.4 Ma (Allmendinger et al., 2005). Another study argued that deep late Miocene to late Pliocene incision called for annual precipitation of at least 125 mm yr^{-1} compared to the present-day <3 mm yr^{-1} (Amundson et al., 2012). It has been inferred that aridity began at 3–4 Ma from supergene mineral deposits (Arancibia et al., 2006), while others showed that deposition of halite deposits slowed in Late Pliocene time because the water table dropped in response to decreased precipitation (Chong Díaz et al., 1999). Aridification was also inferred at ~6.4 Ma when saline lakes developed with further drying near 3.7 Ma, when conglomeratic deposition replaced saline lacustrine sedimentation (Gaupp et al., 1999; Sáez et al., 1999). Decreasing fluvial deposition and increasing deposition of evaporites between ~6 Ma and 4–3 Ma indicated onset of hyperaridification at 4–3 Ma (Hartley & Chong, 2002). Another study however, challenged inferences of that study (Hartley & Chong, 2002) and others, but they worked in a region of higher elevation and assigned surface uplift to environmental changes (Rech et al., 2006).

On the east side of the Andes in Argentina, aridification was reported at 3–2.5 Ma and since 3 Ma (Kleinert & Strecker, 2001; Sobel & Strecker, 2003). Although the authors of those studies (Kleinert & Strecker, 2001; Sobel & Strecker, 2003) ascribed this aridification to tectonic processes and the emergence of rain shadows, we allow it to have been a regional phenomenon.

We are aware of only one study closer to the equator and nearer ODP Site 1237 than those discussed above. From the Central Andes of southern Peru, paleobotanical fossils, including pollen, spores, wood, leaves, and fruits, imply a somewhat higher mean annual precipitation, 620–1121 mm, at 4.8 Ma than today's ~500–800 mm (Martínez et al., 2020).

Appendix A3: West Africa (North)

Much of the evidence in this region is derived from sediment deposited off the west coast of Africa and sampled by cores of the Ocean Drilling Program. Consequently, assigning a location to the source of sediment is necessarily imprecise. A second group of observations comes from Megalake Chad, a large ancient lake in central Africa, and hence thousands of kilometers from the coast, where the oldest hominid fossils have been found apparently near lakeside environments (Brunet et al., 2002).

Fossil pollen deposited in ODP Site 658 suggest wetter conditions before 3.5 Ma than since (Leroy & Dupont, 1994, 1997). Moreover, it was noted that "tropical forests and mangrove swamps reached Cape Blanc, 5°N of the present distribution" (Leroy & Dupont, 1994). These observations seem to apply only to the coast of west Africa, where such forests and swamps live today. From increasing amounts of dust deposited in several ODP sites near the coast, increasing aridity was inferred in West Africa since 7.4 Ma and especially

since 4.0–3.6 Ma (Tiedemann et al., 1989). That dust almost surely comes from desert regions inland from the coast. It was also shown that the onset or acceleration of dust deposition migrated northward (Tiedemann et al., 1989).

For the Lake Chad region, fossil pollen suggest a "wooded humid habitat" if not rainforest, but little grass at ~7 Ma, with gallery forests at 3.0–3.5 Ma (Brunet et al., 1995), where desert conditions now prevail (Bonnefille, 2010). A wealth of observations suggest a huge lake, Megalake Chad, in a wetter late Miocene and early Pliocene climate than since that time: widespread lacustrine sediment (Moussa et al., 2016); fossils of freshwater fish (Otero et al., 2009a, 2009b, 2010), including fish as large as 1 m in length (Vignaud et al., 2002); diatoms and phytoliths (Novello et al., 2015); trace fossils of burrowing animals (Duringer et al., 2000; Schuster et al., 2009); fossil mammals—primates, rodents, elephants, equids, and bovids—(Vignaud et al., 2002), aquatic birds (Louchart et al., 2004); and shifts in $\delta^{13}C$ values in tooth enamel that suggest a shift from mixed C_3/C_4 plant communities to mostly C_4 plants and more open grasslands since 3.6 Ma (Zazzo et al., 2000).

Megalake Chad seems to have been vast, occupying a substantial fraction (~30%) of the drainage basin that is ~2.5×10^6 km^2 in extent and much deeper than the present lake (Schuster et al., 2009). An area of 700,000 km^2 has been suggested for the Mio-Pliocene lake (Griffin, 2006). In late Miocene and early Pliocene time, the lake drained into the Mediterranean (Gladstone et al., 2007; Griffin, 2002, 2006). It has been reported that before ~3 Ma, vast lakes also covered Libya to the north, through which Megalake Chad drained (Drake et al., 2008). Differences among $\delta^{18}O$ from freshwater fishes have also been used to infer a shift from less to more arid conditions between 7 and 3.6 Ma (Otero et al., 2011). Maintaining such a large lake required much heavier rainfall than today's mean annual average of 350 mm, with at least 650 mm needed to maintain a much smaller lake during the early Holocene (Kutzbach, 1980).

Appendix A4: Namibia-Angola (Southwestern Africa)

As for West Africa, several studies, including pollen deposited offshore, call for wetter late Miocene and Pliocene climates along the Atlantic side of southern Africa than the more arid climate today, though again only with qualitative evidence (Scott, 1995). From Site 1082 (21°S), grassy savannas apparently prevailed before 3 Ma, with subsequent aridification and desertification by 2.2 Ma (Dupont, 2006; Dupont et al., 2005). From Site 1085 (29°S), it was argued that "After 4.5 Ma, grasslands changed into semi-desert shrubland...," although no data was reported since 3 Ma (Dupont et al., 2013). From fossil eggshells found in six sites along the southwest coast of Namibia between 25° and 29°S, a change in $\delta^{13}C$ since 3.6 Ma was associated with a switch from mostly C_3 to C_4 plants, and therefore with aridification (Segalen et al., 2002). Farther south, near the coast of Namaqualand (between ~28.5°S and 30.5°S), several have inferred wetter Pliocene than present climates: from past thicket vegetation (Cowling et al., 2005), fossil mammals (Pickford & Senut, 1997; Pickford et al., 1999), and pollen suggestive of sclerophyllous woodland and grassland (Tankard & Rogers, 1978).

Within southern Africa, at the Makapansgat hominid site, pollen suggest a more forested environment between 3.33 and 2.58 Ma (Cadman & Rayner, 1989; Sloggett, 2016), with two to three times more annual rainfall than today's 700 mm (Rayner et al., 1993). Fossil wood dated at 2.6–2.8 Ma in the Sterkfontein Cave hominid site in South Africa was used to infer higher Pliocene than present-day rainfall (Bamford, 1999).

Data Availability Statement

All GCM input files and post-processing scripts are available under https://osf.io/hz3vx/.

Acknowledgments
The authors thank Dr. Kevin Hodges for guidance on using the TRACK program. We thank Dr. Marci Robinson, an anonymous reviewer, and associate editor Dr. Alex Farnsworth for their helpful comments. Eli Tziperman thanks the Weizmann Institute for its hospitality during parts of this work. We would like to acknowledge high-performance computing support from Cheyenne (https://doi.org/10.5065/D6RX99HX) provided by NCAR's Computational and Information Systems Laboratory, sponsored by the National Science Foundation. Eli Tziperman and Minmin Fu were supported by the NSF Climate Dynamics program grants AGS-1924538, AGS-1826635, and by the Harvard-UTEC fund; Peter Molnar is supported by AGS-1740536; Mark A. Cane is supported by NSF award OCE-1657209.

References

Allen, J. S. (1980). Models of wind-driven currents on the continental shelf. *Annual Review of Fluid Mechanics*, *12*(1), 389–433. https://doi.org/10.1146/annurev.fl.12.010180.002133

Allmendinger, R. W., González, G., Yu, J., Hoke, G., & Isacks, B. (2005). Trench-parallel shortening in the Northern Chilean Forearc: Tectonic and climatic implications. *Geological Society of America Bulletin*, *117*(1–2), 89–104. https://doi.org/10.1130/b25505.1

Amundson, R., Dietrich, W., Bellugi, D., Ewing, S., Nishiizumi, K., Chong, G., & Caffee, M. (2012). Geomorphologic evidence for the late Pliocene onset of hyperaridity in the Atacama Desert. *Bulletin*, *124*(7–8), 1048–1070. https://doi.org/10.1130/b30445.1

Arancibia, G., Matthews, S. J., & de Arce, C. P. (2006). K–Ar and 40Ar/39Ar geochronology of supergene processes in the Atacama Desert, Northern Chile: Tectonic and climatic relations. *Journal of the Geological Society*, *163*(1), 107–118. https://doi.org/10.1144/0016-764904-161

Arnold, N. P., & Tziperman, E. (2016). Reductions in midlatitude upwelling-favorable winds implied by weaker large-scale Pliocene SST gradients. *Paleoceanography*, *31*(1), 27–39. https://doi.org/10.1002/2015pa002806

Arnold, N. P., Tziperman, E., & Farrell, B. F. (2012). Abrupt transition to strong superrotation driven by equatorial wave resonance in an idealized GCM. *Journal of the Atmospheric Sciences*, *69*, 626–640. https://doi.org/10.1175/JAS-D-11-0136.1

Bakun, A., & Nelson, C. S. (1991). The seasonal cycle of wind-stress curl in subtropical eastern boundary current regions. *Journal of Physical Oceanography*, *21*(12), 1815–1834. https://doi.org/10.1175/1520-0485(1991)021<1815:tscows>2.0.co;2

Bamford, M. (1999). Pliocene fossil woods from an early hominid cave deposit, Sterkfontein, South Africa. *South African Journal of Science*, *95*(5), 231–237.

Bartolino, J. R., & Cole, J. C. (2002). Chapter 3, Geology of the Santa Fe Group aquifer system. In *Ground-Water Resources of the Middle Rio Grande Basin* (Vol. 1222, pp. 23–40). USGS Water-Resources Circular.

Boccaletti, G., Pacanowski, R. C., Philander, S., Fedorov, A., & Fedorov, A. V. (2004). The thermal structure of the upper ocean. *Journal of Physical Oceanography*, *34*(4), 888–902. https://doi.org/10.1175/1520-0485(2004)034<0888:ttsotu>2.0.co;2

Bonnefille, R. (2010). Cenozoic vegetation, climate changes and hominid evolution in tropical Africa. *Global and Planetary Change*, *72*(4), 390–411. https://doi.org/10.1016/j.gloplacha.2010.01.015

Botsford, L. W., Lawrence, C. A., Dever, E. P., Hastings, A., & Largier, J. (2006). Effects of variable winds on biological productivity on continental shelves in coastal upwelling systems. *Deep Sea Research Part II: Topical Studies in Oceanography*, *53*(25–26), 3116–3140. https://doi.org/10.1016/j.dsr2.2006.07.011

Bowen, I. S. (1926). The ratio of heat losses by conduction and by evaporation from any water surface. *Physical Review*, *27*(6), 779–787. https://doi.org/10.1103/physrev.27.779

Brierley, C. M., Burls, N., Ravelo, C., & Fedorov, A. (2015). Pliocene warmth and gradients. *Nature Geoscience*, *8*(6), 419–420. https://doi.org/10.1038/ngeo2444

Brierley, C. M., Fedorov, A. V., Liu, Z., Herbert, T. D., Lawrence, K. T., & LaRiviere, J. P. (2009). Greatly expanded tropical warm pool and weakened Hadley circulation in the early Pliocene. *Science*, *323*(5922), 1714–1718. https://doi.org/10.1126/science.1167625

Brister, B. S., & Gries, R. R. (1994). Tertiary stratigraphy and tectonic development of the Alamosa basin (northern San Luis Basin), Rio Grande rift, south-central Colorado. In G. R. Keller, & S. M. Cather (Eds.), *Basins of the Rio Grande rift: Structure, stratigraphy, and tectonic setting* (pp. 39–58): Geological Society of America Special Paper 291. https://doi.org/10.1130/spe291-p39

Brown, R. W. (1949). Pliocene plants from Cachee (sic) Valley, Utah. *Journal of the Washington Academy of Sciences*, *39*(7), 224–229.

Brunet, M., Beauvilain, A., Coppens, Y., Heintz, E., Moutaye, A. H., & Pilbeam, D. (1995). The first australopithecine 2,500 kilometres west of the Rift Valley (Chad). *Nature*, *378*(6554), 273–275. https://doi.org/10.1038/378273a0

Brunet, M., Guy, F., Pilbeam, D., Mackaye, H. T., Likius, A., Ahounta, D., et al. (2002). A new hominid from the Upper Miocene of Chad, Central Africa. *Nature*, *418*(6894), 145–151. https://doi.org/10.1038/nature00879

Burls, N. J., & Fedorov, A. V. (2017). Wetter subtropics in a warmer world: Contrasting past and future hydrological cycles. *Proceedings of the National Academy of Sciences*, *114*(49), 12888–12893. https://doi.org/10.1073/pnas.1703421114

Cadman, A., & Rayner, R. J. (1989). Climatic change and the appearance of Australopithecus africanus in the Makapansgat sediments. *Journal of Human Evolution*, *18*(2), 107–113. https://doi.org/10.1016/0047-2484(89)90065-1

Chong Díaz, G., Mendoza, M., García-Veigas, J., Pueyo, J. J., & Turner, P. (1999). Evolution and geochemical signatures in a Neogene forearc evaporitic basin: The Salar Grande (Central Andes of Chile). *Palaeogeography, Palaeoclimatology, Palaeoecology*, *151*(1–3), 39–54.

Collins, E. W., & Raney, J. A. (1994). Tertiary and Quaternary tectonics of the Hueco bolson, Trans-Pecos Texas and Chihuahua, Mexico. In G. R. Keller, & S. M. Cather (Eds.), *Tertiary and quaternary tectonics of the Hueco bolson, trans-pecos Texas and Chihuahua, Mexico. Basins of the Rio Grande rift: Structure, stratigraphy, and tectonic setting* (pp. 265–282): Geological Society of America Special Paper 291. https://doi.org/10.1130/spe291-p265

Connell, S. D., Smith, G. A., Geissman, J. W., & McIntosh, W. C. (2013). In M. R. Hudson, & V. J. S Grauch (Eds.), *Climatic controls on nonmarine depositional sequences in the Albuquerque Basin, Rio Grande rift, north-central New Mexico. New Perspectives on Rio Grande Rift Basins: From Tectonics to Groundwater* (Vol. 494, pp. 383–425). Geological Society of America Special Paper.

Cowling, R. M., Procheş, Ş., Vlok, J. H. J., & Van Staden, J. (2005). On the origin of southern African subtropical thicket vegetation. *South African Journal of Botany*, *71*(1), 1–23. https://doi.org/10.1016/s0254-6299(15)30144-7

Davis, O. K., & Moutoux, T. E. (1998). Tertiary and Quaternary vegetation history of the Great Salt Lake, Utah, USA. *Journal of Paleolimnology*, *19*(4), 417–427. https://doi.org/10.1023/a:1007959203433

Dekens, P. S., Ravelo, A. C., & McCarthy, M. D. (2007). Warm upwelling regions in the Pliocene warm period. *Paleoceanography*, *22*(3). https://doi.org/10.1029/2006pa001394

Dowsett, H. J., Foley, K. M., Stoll, D. K., Chandler, M. A., Sohl, L. E., Bentsen, M., & Zhang, Z. (2013). Sea surface temperature of the mid-Piacenzian ocean: A data-model comparison. *Scientific Reports*, *3*(1), 1–8. https://doi.org/10.1038/srep02013

Dowsett, H. J., Haywood, A. M., Valdes, P. J., Robinson, M. M., Lunt, D. J., Hill, D. J., & Foley, K. M. (2011). Sea surface temperatures of the mid-Piacenzian Warm Period: A comparison of PRISM3 and HadCM3. *Palaeogeography, Palaeoclimatology, Palaeoecology*, *309*(1–2), 83–91. https://doi.org/10.1016/j.palaeo.2011.03.016

Dowsett, H. J., & Robinson, M. M. (2009). Mid-Pliocene equatorial sea surface temperature reconstruction: A multi-proxy perspective. *Philosophical Transactions of the Royal Society*, *367*(1886), 109–125. https://doi.org/10.1098/rsta.2008.0206

Drake, N. A., El-Hawat, A. S., Turner, P., Armitage, S. J., Salem, M. J., White, K. H., & McLaren, S. (2008). Palaeohydrology of the Fazzan Basin and surrounding regions: The last 7 million years. *Palaeogeography, Palaeoclimatology, Palaeoecology*, *263*(3–4), 131–145. https://doi.org/10.1016/j.palaeo.2008.02.005

Dugdale, R. C., Wilkerson, F. P., Hogue, V. E., & Marchi, A. (2006). Nutrient controls on new production in the Bodega Bay, California, coastal upwelling plume. *Deep Sea Research Part II: Topical Studies in Oceanography*, *53*(25–26), 3049–3062. https://doi.org/10.1016/j.dsr2.2006.07.009

Dupont, L. M. (2006). Late Pliocene vegetation and climate in Namibia (southern Africa) derived from palynology of ODP Site 1082. *Geochemistry, Geophysics, Geosystems*, *7*(5), Q05007. https://doi.org/10.1029/2005gc001208

Dupont, L. M., Donner, B., Vidal, L., Pérez, E. M., & Wefer, G. (2005). Linking desert evolution and coastal upwelling: Pliocene climate change in Namibia. *Geology*, *33*(6), 461–464. https://doi.org/10.1130/g21401.1

Dupont, L. M., Rommerskirchen, F., Mollenhauer, G., & Schefuß, E. (2013). Miocene to Pliocene changes in South African hydrology and vegetation in relation to the expansion of C4 plants. *Earth and Planetary Science Letters*, *375*, 408–417. https://doi.org/10.1016/j.epsl.2013.06.005

Duringer, P., Brunet, M., Cambefort, Y., Beauvilain, A., Mackaye, H. T., Vignaud, P., & Schuster, M. (2000). Des boules de bousiers fossiles et leurs terriers dans les sites à Australopithèques du Pliocène tchadien. *Bulletin de la Societe Geologique de France*, *171*(2), 259–269. https://doi.org/10.2113/171.2.259

Enriquez, A. G., & Friehe, C. A. (1995). Effects of wind stress and wind stress curl variability on coastal upwelling. *Journal of Physical Oceanography*, *25*(7), 1651–1671. https://doi.org/10.1175/1520-0485(1995)025<1651:eowsaw>2.0.co;2

Fedorov, A. V., Brierley, C. M., & Emanuel, K. (2010). Tropical cyclones and permanent El Niño in the early Pliocene epoch. *Nature*, *463*(7284), 1066–1070. https://doi.org/10.1038/nature08831

Fedorov, A. V., Brierley, C. M., Lawrence, K. T., Liu, Z., Dekens, P. S., & Ravelo, A. C. (2013). Patterns and mechanisms of early Pliocene warmth. *Nature*, *496*(7443), 43–49. https://doi.org/10.1038/nature12003

Fedorov, A. V., Dekens, P. S., McCarthy, M., Ravelo, A. C., DeMenocal, P. B., Barreiro, M., & Philander, S. G. (2006). The Pliocene paradox (mechanisms for a permanent El Niño). *Science*, *312*(5779), 1485–1489. https://doi.org/10.1126/science.1122666

Foley, K. M., & Dowsett, H. J. (2019). *Community sourced mid-Piacenzian sea surface temperature (SST) data*. US Geological Survey data release. https://doi.org/10.5066/P9YP3DTV

Forester, R. M. (1991). Pliocene-climate history of the western United States derived from lacustrine ostracodes. *Quaternary Science Reviews*, *10*(2–3), 133–146. https://doi.org/10.1016/0277-3791(91)90014-l

Galusha, T., & Blick, J. C. (1971). Stratigraphy of the Santa Fe Group, New Mexico. *Bulletin of the American Museum of Natural History*, *144*, 1–128.article 1.

García-Reyes, M., & Largier, J. (2010). Observations of increased wind-driven coastal upwelling off central California. *Journal of Geophysical Research: Oceans*, *115*(C4), C04011. https://doi.org/10.1029/2009jc005576

Gaupp, R., Kött, A., & Wörner, G. (1999). Palaeoclimatic implications of Mio–Pliocene sedimentation in the high-altitude intra-arc Lauca Basin of northern Chile. *Palaeogeography, Palaeoclimatology, Palaeoecology*, *151*(1–3), 79–100. https://doi.org/10.1016/s0031-0182(99)00017-6

Gladstone, R., Flecker, R., Valdes, P., Lunt, D., & Markwick, P. (2007). The Mediterranean hydrologic budget from a Late Miocene global climate simulation. *Palaeogeography, Palaeoclimatology, Palaeoecology*, *251*(2), 254–267. https://doi.org/10.1016/j.palaeo.2007.03.050

Griffin, D. L. (2002). Aridity and humidity: Two aspects of the late Miocene climate of North Africa and the Mediterranean. *Palaeogeography, Palaeoclimatology, Palaeoecology*, *182*(1–2), 65–91. https://doi.org/10.1016/s0031-0182(01)00453-9

Griffin, D. L. (2006). The late Neogene Sahabi rivers of the Sahara and their climatic and environmental implications for the Chad Basin. *Journal of the Geological Society*, *163*(6), 905–921. https://doi.org/10.1144/0016-76492005-049

Hager, M. W. (1974). *Late Pliocene and Pleistocene History of the Donnelly Ranch Vertebrate Site, Southeastern Colorado* (Vol. 2, p. 62). University of Wyoming.Contributions to Geology - Special Paper.

Hartley, A. J., & Chong, G. (2002). Late Pliocene age for the Atacama Desert: Implications for the desertification of western South America. *Geology*, *30*(1), 43–46. https://doi.org/10.1130/0091-7613(2002)030<0043:lpafta>2.0.co;2

Hay, R. L., Pexton, R. E., Teague, T. T., & Kurtis Kyser, T. (1986). Spring-related carbonate rocks, Mg clays, and associated minerals in Pliocene deposits of the Amargosa Desert, Nevada and California. *Geological Society of America Bulletin*, *97*(12), 1488–1503. https://doi.org/10.1130/0016-7606(1986)97<1488:scrmca>2.0.co;2

Haywood, A. M., Dowsett, H. J., Otto-Bliesner, B., Chandler, M. A., Dolan, A. M., Hill, D. J., et al. (2010). Pliocene model intercomparison project (PlioMIP): Experimental design and boundary conditions (experiment 1). *Geoscientific Model Development*, *3*(1), 227–242. https://doi.org/10.5194/gmd-3-227-2010

Haywood, A. M., Tindall, J. C., Dowsett, H. J., Dolan, A. M., Foley, K. M., Hunter, S. J., et al. (2020). The Pliocene Model Intercomparison Project Phase 2: Large-scale climate features and climate sensitivity. *Climate of the Past*, *16*(6), 2095–2123. https://doi.org/10.5194/cp-16-2095-2020

Herbert, T. D., Lawrence, K. T., Tzanova, A., Peterson, L. C., Caballero-Gill, R., & Kelly, C. S. (2016). Late Miocene global cooling and the rise of modern ecosystems. *Nature Geoscience*, *9*(11), 843–847. https://doi.org/10.1038/ngeo2813

Herbert, T. D., & Schuffert, J. D. (1998). Alkenone unsaturation estimates of late Miocene through late Pliocene sea-surface temperatures at Site 958. *Proceedings of the Ocean Drilling Program-Scientific Results*, *159T*, 17–21. https://doi.org/10.2973/odp.proc.sr.159t.063.1998

Hodges, K. I. (1994). A general method for tracking analysis and its application to meteorological data. *Monthly Weather Review*, *122*(11), 2573–2586. https://doi.org/10.1175/1520-0493(1994)122<2573:agmfta>2.0.co;2

Hodges, K. I. (1996). Spherical nonparametric estimators applied to the UGAMP model integration for AMIP. *Monthly Weather Review*, *124*(12), 2914–2932. https://doi.org/10.1175/1520-0493(1996)124<2914:sneatt>2.0.co;2

Hurlburt, H. E., & Thompson, J. D. (1973). Coastal upwelling on a β-plane. *Journal of Physical Oceanography*, *3*(1), 16–32. https://doi.org/10.1175/1520-0485(1973)003<0016:cuoap>2.0.co;2

Hurrell, J. W., Hack, J. J., Shea, D., Caron, J. M., & Rosinski, J. (2008). A new sea surface temperature and sea ice boundary dataset for the Community Atmosphere Model. *Journal of Climate*, *21*(19), 5145–5153. https://doi.org/10.1175/2008jcli2292.1

Ibarra, D. E., Oster, J. L., Winnick, M. J., Caves Rugenstein, J. K., Byrne, M. P., & Chamberlain, C. P. (2018). Warm and cold wet states in the western United States during the Pliocene–Pleistocene. *Geology*, *46*(4), 355–358. https://doi.org/10.1130/g39962.1

Israde-Alcántara, I., Miller, W. E., Garduño-Monroy, V. H., Barron, J., & Rodriguez-Pascua, M. A. (2010). Palaeoenvironmental significance of diatom and vertebrate fossils from Late Cenozoic tectonic basins in west-central México: A review. *Quaternary International*, *219*(1–2), 79–94. https://doi.org/10.1016/j.quaint.2010.01.012

Kleinert, K., & Strecker, M. R. (2001). Climate change in response to orographic barrier uplift: Paleosol and stable isotope evidence from the late Neogene Santa Maria basin, northwestern Argentina. *Geological Society of America Bulletin*, *113*(6), 728–742. https://doi.org/10.1130/0016-7606(2001)113<0728:ccirto>2.0.co;2

Knott, J. R., Machette, M. N., Klinger, R. E., Sarna-Wojcicki, A. M., Liddicoat, J. C., Tinsley, J. C., III, et al. (2008). Reconstructing late Pliocene to middle Pleistocene Death Valley lakes and river systems as a test of pupfish (Cyprinodontidae) dispersal hypotheses. In *Late Cenozoic Drainage History of the Southwestern Great Basin and Lower Colorado River Region: Geologic and Biotic Perspectives* (Vol. 439, pp. 1–26). https://doi.org/10.1130/2008.2439(01)

Knott, J. R., Machette, M. N., Wan, E., Klinger, R. E., Liddicoat, J. C., Sarna-Wojcicki, A. M., & Weamer, V. M. (2018). Late Neogene–Quaternary tephrochronology, stratigraphy, and paleoclimate of Death Valley, California, USA. *Bulletin*, *130*(7–8), 1231–1255. https://doi.org/10.1130/b31690.1

Kowalewska, A., & Cohen, A. S. (1998). Reconstruction of paleoenvironments of the Great Salt Lake Basin during the late Cenozoic. *Journal of Paleolimnology*, *20*(4), 381–407. https://doi.org/10.1023/a:1008053505320
Kürschner, W. M., van der Burgh, J., Visscher, H., & Dilcher, D. L. (1996). Oak leaves as biosensors of late Neogene and early Pleistocene paleoatmospheric CO_2 concentrations. *Marine Micropaleontology*, *27*(1–4), 299–312. https://doi.org/10.1016/0377-8398(95)00067-4
Kutzbach, J. E. (1980). Estimates of past climate at Paleolake Chad, North Africa, based on a hydrological and energy-balance model. *Quaternary Research*, *14*(2), 210–223. https://doi.org/10.1016/0033-5894(80)90049-6
Largier, J. L., Lawrence, C. A., Roughan, M., Kaplan, D. M., Dever, E. P., Dorman, C. E., & Koračin, L. (2006). WEST: A northern California study of the role of wind-driven transport in the productivity of coastal plankton communities. *Deep Sea Research Part II: Topical Studies in Oceanography*, *53*(25–26), 2833–2849. https://doi.org/10.1016/j.dsr2.2006.08.018
LaRiviere, J. P., Ravelo, A. C., Crimmins, A., Dekens, P. S., Ford, H. L., Lyle, M., & Wara, M. W. (2012). Late Miocene decoupling of oceanic warmth and atmospheric carbon dioxide forcing. *Nature*, *486*(7401), 97–100. https://doi.org/10.1038/nature11200
Lawrence, D. M., Oleson, K. W., Flanner, M. G., Thornton, P. E., Swenson, S. C., Lawrence, P. J., & Slater, A. G. (2011). Parameterization improvements and functional and structural advances in Version 4 of the Community Land Model. *Journal of Advances in Modeling Earth Systems*, *3*(1), M03001. https://doi.org/10.1029/2011ms00045
Lawrence, K. T., Liu, Z., & Herbert, T. D. (2006). Evolution of the eastern tropical Pacific through Plio-Pleistocene glaciation. *Science*, *312*(5770), 79–83. https://doi.org/10.1126/science.1120395
Laymon, C. A., & Quattrochi, D. A. (2004). Estimating spatially distributed surface fluxes in a semi-arid Great Basin desert using Landsat TM thermal data. In *Thermal remote sensing in land surface processing* (pp. 155–181). CRC Press. https://doi.org/10.1201/9780203502174-c5
Leopold, E. B., & Wright, V. C. (1985). Pollen profiles of the Plio-Pleistocene transition in the Snake River plain, Idaho. In *Late Cenozoic History of the Pacific Northwest. Edited by CJ Smiley, CJ Pacific Division* (pp. 323–348). , American Academy of Sciences.
Leroy, S., & Dupont, L. (1994). Development of vegetation and continental aridity in northwestern Africa during the Late Pliocene: The pollen record of ODP Site 658. *Palaeogeography, Palaeoclimatology, Palaeoecology*, *109*(2–4), 295–316. https://doi.org/10.1016/0031-0182(94)90181-3
Leroy, S., & Dupont, L. M. (1997). Marine palynology of the ODP Site 658 (NW Africa) and its contribution to the stratigraphy of Late Pliocene. *Geobios*, *30*(3), 351–359. https://doi.org/10.1016/s0016-6995(97)80194-5
Li, Z., Luo, Y., Arnold, N., & Tziperman, E. (2019). Reductions in strong upwelling-favorable wind events in the Pliocene. *Paleoceanography and Paleoclimatology*, *34*(12), 1931–1944. https://doi.org/10.1029/2019pa003760
Louchart, A., Mourer-Chauviré, C., Mackaye, H. T., Likius, A., Vignaud, P., & Brunet, M. (2004). Les oiseaux du Pliocène inférieur du Djourab, Tchad, Afrique centrale. *Bulletin de la Societe Geologique de France*, *175*(4), 413–421. https://doi.org/10.2113/175.4.413
Machette, M. N., Thompson, R. A., Marchetti, D. W., & Smith, R. S. (2013). Evolution of ancient Lake Alamosa and integration of the Rio Grande during the Pliocene and Pleistocene. *Geological Society of America Special Paper*, *494*, 1–20. https://doi.org/10.1130/2013.2494(01)
Malek, E., Bingham, G. E., & McCurdy, G. D. (1990). Evapotranspiration from the margin and moist playa of a closed desert valley. *Journal of Hydrology*, *120*(1–4), 15–34. https://doi.org/10.1016/0022-1694(90)90139-o
Marlow, J. R., Lange, C. B., Wefer, G., & Rosell-Melé, A. (2000). Upwelling intensification as part of the Pliocene-Pleistocene climate transition. *Science*, *290*(5500), 2288–2291.
Marshall, J., & Plumb, R. A. (2008). *Atmosphere, ocean, and climate dynamics*: Elsevier Academic Press.
Martínez, C., Jaramillo, C., Correa-Metrío, A., Crepet, W., Moreno, J. E., Aliaga, A., et al. (2020). Neogene precipitation, vegetation, and elevation history of the Central Andean Plateau. *Science Advances*, *6*(35), eaaz4724. https://doi.org/10.1126/sciadv.aaz4724
McClellan, P. H., & Smith, G. R. (2020). *Late Miocene Fishes on the Cache Valley Member, Salt Lake Formation, Utah and Idaho* (Vol. 208, p. 54). Miscellaneous Publications, Museum of Zoology, University of Michigan.
McClymont, E. L., Ford, H. L., Ho, S. L., Tindall, J. C., Haywood, A. M., Alonso-Garcia, M., et al. (2020). Lessons from a high-CO_2 world: An ocean view from ~3 million years ago. *Climate of the Past*, *16*(4), 1599–1615. https://doi.org/10.5194/cp-16-1599-2020
Miller, M. D., & Tziperman, E. (2017). The effect of changes in surface winds and ocean stratification on coastal upwelling and sea surface temperatures in the Pliocene. *Paleoceanography*, *32*(4), 371–383. https://doi.org/10.1002/2016pa002996
Minnich, R. A. (2007). 2. Climate, Paleoclimate, and Paleovegetation. In *Terrestrial vegetation of California* (3rd ed., pp. 43–70). University of California Press. https://doi.org/10.1525/california/9780520249554.003.0002
Molnar, P., & Cane, M. A. (2002). El Niño's tropical climate and teleconnections as a blueprint for pre-Ice Age climates. *Paleoceanography*, *17*, 1–11. https://doi.org/10.1029/2001pa000663
Molnar, P., & Cane, M. A. (2007). Early Pliocene (pre-Ice Age) El Niño-like global climate: Which El Niño? *Geosphere*, *3*(5), 337–365. https://doi.org/10.1130/ges00103.1
Moussa, A., Novello, A., Lebatard, A.-E., Decarreau, A., Fontaine, C., Barboni, D., et al. (2016). Lake Chad sedimentation and environments during the late Miocene and Pliocene: New evidence from mineralogy and chemistry of the Bol core sediments. *Journal of African Earth Sciences*, *118*, 192–204. https://doi.org/10.1016/j.jafrearsci.2016.02.023
Neale, R. B., Chen, C.-C., Gettelman, A., Lauritzen, P. H., Park, S., & Williamson, D. L. (2012). Description of the NCAR community atmosphere model (CAM 5.0). In NCAR Technology. Note NCAR/TN-486+ STR.
Novello, A., Lebatard, A.-E., Moussa, A., Barboni, D., Sylvestre, F., Bourlès, D. L., et al. (2015). Diatom, phytolith, and pollen records from a 10Be/9Be dated lacustrine succession in the Chad basin: Insight on the Miocene–Pliocene paleoenvironmental changes in Central Africa. *Palaeogeography, Palaeoclimatology, Palaeoecology*, *430*, 85–103. https://doi.org/10.1016/j.palaeo.2015.04.013
O'Brien, C. L., Foster, G. L., Martínez-Botí, M. A., Abell, R., Rae, J. W., & Pancost, R. D. (2014). High sea surface temperatures in tropical warm pools during the Pliocene. *Nature Geoscience*, *7*(8), 606–611.
Otero, O., Lécuyer, C., Fourel, F., Martineau, F., Mackaye, H. T., Vignaud, P., & Brunet, M. (2011). Freshwater fish δ18O indicates a Messinian change of the precipitation regime in Central Africa. *Geology*, *39*(5), 435–438. https://doi.org/10.1130/g31212.1
Otero, O., Pinton, A., Mackaye, H. T., Likius, A., Vignaud, P., & Brunet, M. (2009a). First description of a Pliocene ichthyofauna from Central Africa (site KL2, Kolle area, Eastern Djurab, Chad): What do we learn? *Journal of African Earth Sciences*, *54*(3–4), 62–74. https://doi.org/10.1016/j.jafrearsci.2009.03.004
Otero, O., Pinton, A., Mackaye, H. T., Likius, A., Vignaud, P., & Brunet, M. (2009b). Fishes and palaeogeography of the African drainage basins: Relationships between Chad and neighbouring basins throughout the Mio-Pliocene. *Palaeogeography, Palaeoclimatology, Palaeoecology*, *274*(3–4), 134–139. https://doi.org/10.1016/j.palaeo.2009.01.005
Otero, O., Pinton, A., Mackaye, H. T., Likius, A., Vignaud, P., & Brunet, M. (2010). The early/late Pliocene ichthyofauna from Koro-Toro, Eastern Djurab, Chad. *Geobios*, *43*(2), 241–251. https://doi.org/10.1016/j.geobios.2009.10.003
Pagani, M., Liu, Z., LaRiviere, J., & Ravelo, A. C. (2010). High Earth-system climate sensitivity determined from Pliocene carbon dioxide concentrations. *Nature Geoscience*, *3*(1), 27–30. https://doi.org/10.1038/ngeo724

Philander, S. G., & Fedorov, A. V. (2003). Role of tropics in changing the response to Milankovich forcing some three million years ago. *Paleoceanography*, *18*(2). https://doi.org/10.1029/2002pa000837
Pickford, M., Eisenmann, V., & Senut, B. (1999). Timing of landscape development and calcrete genesis in northern Namaqualand, South Africa. *South African Journal of Science*, *95*(8), 357–359.
Pickford, M., & Senut, B. (1997). Cainozoic mammals from coastal Namaqualand, South Africa. *Paleontology of Africa*, *34*, 199–217.
Pound, M. J., Tindall, J., Pickering, S. J., Haywood, A. M., Dowsett, H. J., & Salzmann, U. (2014). Late Pliocene lakes and soils: A global data set for the analysis of climate feedbacks in a warmer world. *Climate of the Past*, *10*(1), 167–180. https://doi.org/10.5194/cp-10-167-2014
Ravelo, A. C., Dekens, P. S., & McCarthy, M. (2006). Evidence for El Niño-like conditions during the Pliocene. *Geological Society of America Today*, *16*(3), 4. https://doi.org/10.1130/1052-5173(2006)016<4:efenlc>2.0.co;2
Ravelo, A. C., Lawrence, K. T., Fedorov, A., & Ford, H. L (2014). Comment on "A 12-million-year temperature history of the tropical Pacific Ocean". *Science*, *346*(6216), 1467–1467. https://doi.org/10.1126/science.1257618
Raymo, M. E., Grant, B., Horowitz, M., & Rau, G. H. (1996). Mid-Pliocene warmth: Stronger greenhouse and stronger conveyor. *Marine Micropaleontology*, *27*(1–4), 313–326. https://doi.org/10.1016/0377-8398(95)00048-8
Rayner, R. J., Moon, B. P., & Masters, J. C. (1993). The Makapansgat australopithecine environment. *Journal of Human Evolution*, *24*(3), 219–231. https://doi.org/10.1006/jhev.1993.1016
Rech, J. A., Currie, B. S., Michalski, G., & Cowan, A. M. (2006). Neogene climate change and uplift in the Atacama Desert, Chile. *Geology*, *34*(9), 761–764. https://doi.org/10.1130/g22444.1
Reheis, M. C., Sarna-Wojcicki, A. M., Reynolds, R. L., Repenning, C. A., & Mifflin, M. D. (2002). Pliocene to middle Pleistocene lakes in the western Great Basin: Ages and connections. In R. Hershler, D. B. Madsen, & D. R. Curry (Eds.). *Great basin aquatic systems history*. *Smithsonian Contributions to the Earth Sciences* (Vol. 33, pp. 53–108).
Remeika, P., Fischbein, I. W., & Fischbein, S. A. (1988). Lower Pliocene petrified wood from the Palm Spring Formation, Anza Borrego Desert State Park, California. *Review of Palaeobotany and Palynology*, *56*(3–4), 183–198. https://doi.org/10.1016/0034-6667(88)90057-7
Renault, L., Dewitte, B., Marchesiello, P., Illig, S., Echevin, V., Cambon, G., & Ayers, J. K. (2012). Upwelling response to atmospheric coastal jets off central Chile: A modeling study of the October 2000 event. *Journal of Geophysical Research: Oceans*, *117*(C2), C02030. https://doi.org/10.1029/2011jc007446
Rodwell, M. J., & Hoskins, B. J. (2001). Subtropical anticyclones and summer monsoons. *Journal of Climate*, *14*(15), 3192–3211. https://doi.org/10.1175/1520-0442(2001)014<3192:saasm>2.0.co;2
Rosenbloom, N. A., Otto-Bliesner, B. L., Brady, E. C., & Lawrence, P. J. (2013). Simulating the mid-Pliocene Warm Period with the CCSM4 model. *Geoscientific Model Development*, *6*(2), 549–561. https://doi.org/10.5194/gmd-6-549-2013
Sáez, A., Cabrera, L., Jensen, A., & Chong, G. (1999). Late Neogene lacustrine record and palaeogeography in the Quillagua–Llamara basin, Central Andean fore-arc (northern Chile). *Palaeogeography, Palaeoclimatology, Palaeoecology*, *151*(1–3), 5–37. https://doi.org/10.1016/s0031-0182(99)00013-9
Salzmann, U., Haywood, A., Lunt, D., Valdes, P., & Hill, D. (2008). A new global biome reconstruction and data-model comparison for the middle Pliocene. *Global Ecology and Biogeography*, *17*(3), 432–447. https://doi.org/10.1111/j.1466-8238.2008.00381.x
Schuster, M., Duringer, P., Ghienne, J.-F., Roquin, C., Sepulchre, P., Moussa, A., & Brunet, M. (2009). Chad Basin: Paleoenvironments of the Sahara since the Late Miocene. *Comptes Rendus Geoscience*, *341*(8–9), 603–611. https://doi.org/10.1016/j.crte.2009.04.001
Scott, L. (1995). Pollen evidence for vegetational and climatic change in southern Africa during the Neogene and Quaternary. *Paleoclimate and Evolution with Emphasis nn Human Origins*, *1*, 65–76.
Segalen, L., Renard, M., Pickford, M., Senut, B., Cojan, I., Le Callonnec, L., & Rognon, P. (2002). Environmental and climatic evolution of the Namib Desert since the Middle Miocene: The contribution of carbon isotope ratios in ratite eggshells. *Comptes Rendus Geoscience*, *334*(12), 917–924. https://doi.org/10.1016/s1631-0713(02)01837-0
Seki, O., Foster, G. L., Schmidt, D. N., Mackensen, A., Kawamura, K., & Pancost, R. D. (2010). Alkenone and boron-based Pliocene pCO2 records. *Earth and Planetary Science Letters*, *292*(1–2), 201–211. https://doi.org/10.1016/j.epsl.2010.01.037
Sloggett, G. C. (2016). An Analysis of the Plio-Pliestocene Paleoecology of Makapansgat, Limpopo Province, South Africa. *vis-à-vis: Explorations in Anthropology*, *13*(1).
Small, R. J., Curchitser, E., Hedstrom, K., Kauffman, B., & Large, W. G. (2015). The Benguela upwelling system: Quantifying the sensitivity to resolution and coastal wind representation in a global climate model. *Journal of Climate*, *28*(23), 9409–9432. https://doi.org/10.1175/jcli-d-15-0192.1
Smith, G. A. (1994). Climatic influences on continental deposition during late-stage filling of an extensional basin, southeastern Arizona. *Geological Society of America Bulletin*, *106*(9), 1212–1228. https://doi.org/10.1130/0016-7606(1994)106<1212:ciocdd>2.3.co;2
Smith, G. A., Wang, Y., Cerling, T. E., & Geissman, J. W. (1993). Comparison of a paleosol-carbonate isotope record to other records of Pliocene-early Pleistocene climate in the western United States. *Geology*, *21*(8), 691–694. https://doi.org/10.1130/0091-7613(1993)021<0691:coapci>2.3.co;2
Smith, G. I. (1984). Paleohydrologic regimes in the southwestern Great Basin, 0–3.2 my ago, compared with other long records of "global" climate. *Quaternary Research*, *22*(1), 1–17. https://doi.org/10.1016/0033-5894(84)90002-4
Smith, G. R. (1981). Late cenozoic freshwater fishes of North America. *Annual Review of Ecology and Systematics*, *12*(1), 163–193. https://doi.org/10.1146/annurev.es.12.110181.001115
Smith, G. R. (1987). Fish speciation in a western North American Pliocene rift lake. *PALAIOS*, *2*(5), 436–445. https://doi.org/10.2307/3514615
Smith, G. R., & Patterson, W. P. (1994). Mio-pliocene seasonality on the Snake River plain: Comparison of faunal and oxygen isotopic evidence. *Palaeogeography, Palaeoclimatology, Palaeoecology*, *107*(3–4), 291–302. https://doi.org/10.1016/0031-0182(94)90101-5
Sobel, E. R., & Strecker, M. R. (2003). Uplift, exhumation and precipitation: Tectonic and climatic control of Late Cenozoic landscape evolution in the northern Sierras Pampeanas, Argentina. *Basin Research*, *15*(4), 431–451. https://doi.org/10.1046/j.1365-2117.2003.00214.x
Spencer, J. E., Patchett, P. J., Pearthree, P. A., House, P. K., Sarna-Wojcicki, A. M., Wan, E., et al. (2013). Review and analysis of the age and origin of the Pliocene Bouse Formation, lower Colorado River Valley, southwestern USA. *Geosphere*, *9*(3), 444–459. https://doi.org/10.1130/ges00896.1
Steph, S., Tiedemann, R., Prange, M., Groeneveld, J., Schulz, M., Timmermann, A., & Haug, G. H. (2010). Early Pliocene increase in thermohaline overturning: A precondition for the development of the modern equatorial Pacific cold tongue. *Paleoceanography*, *25*(2). https://doi.org/10.1029/2008pa001645
Stuart, C. J., & Willingham, D. L. (1984). Late Tertiary and Quaternary fluvial deposits in the Mesilla and Hueco bolsons, El Paso area, Texas. *Sedimentary Geology*, *38*(1–4), 1–20. https://doi.org/10.1016/0037-0738(84)90072-1
Stull, R. B. (2012). *An Introduction to Boundary Layer Meteorology* (Vol. 13). Springer Science & Business Media.

Sturman, A. P., & McGowan, H. A. (2009). Observations of dry season surface energy exchanges over a desert clay pan, Queensland, Australia. *Journal of Arid Environments*, *73*(1), 74–81. https://doi.org/10.1016/j.jaridenv.2008.08.008

Takahashi, K., & Battisti, D. S. (2007). Processes controlling the mean tropical Pacific precipitation pattern. Part I: The Andes and the eastern Pacific ITCZ. *Journal of Climate*, *20*(14), 3434–3451. https://doi.org/10.1175/jcli4198.1

Tankard, A. J., & Rogers, J. (1978). Late Cenozoic palaeoenvironments on the west coast of southern Africa. *Journal of Biogeography*, *5*, 319–337. https://doi.org/10.2307/3038026

Thompson, R. S. (1991). Pliocene environments and climates in the western United States. *Quaternary Science Reviews*, *10*(2–3), 115–132. https://doi.org/10.1016/0277-3791(91)90013-k

Thompson, R. S. (1992). *Palynological data from a 989-ft (301-m) core of Pliocene and Early Pleistocene sediments from Bruneau, Idaho*. (Vol. 92–713, pp. 1–28). USGS Open File Report. https://doi.org/10.3133/ofr92713

Thompson, R. S. (1996). Pliocene and early Pleistocene environments and climates of the western Snake River Plain, Idaho. *Marine Micropaleontology*, *27*(1–4), 141–156. https://doi.org/10.1016/0377-8398(95)00056-9

Thompson, R. S., & Fleming, R. F. (1996). Middle Pliocene vegetation: Reconstructions, paleoclimatic inferences, and boundary conditions for climate modeling. *Marine Micropaleontology*, *27*(1–4), 27–49. https://doi.org/10.1016/0377-8398(95)00051-8

Tiedemann, R., Sarnthein, M., & Stein, R. (1989). Climatic changes in the western Sahara: Aeolo-marine sediment record of the last 8 million years (sites 657-661). In W. Ruddiman, M. Sarnthein, et al. (Eds.), *Proceedings of the Ocean Drilling Program: Scientific Results* (Vol. 108, pp. 241–277). https://doi.org/10.2973/odp.proc.sr.108.169.1989

Tierney, J. E., Haywood, A. M., Feng, R., Bhattacharya, T., & Otto-Bliesner, B. L. (2019). Pliocene warmth consistent with greenhouse gas forcing. *Geophysical Research Letters*, *46*(15), 9136–9144. https://doi.org/10.1029/2019gl083802

Twine, T. E., Kustas, W., Norman, J., Cook, D., Houser, P., Meyers, T., et al. (2000). Correcting eddy-covariance flux underestimates over a grassland. *Agricultural and Forest Meteorology*, *103*(3), 279–300. https://doi.org/10.1016/s0168-1923(00)00123-4

Tziperman, E., & Farrell, B. (2009). Pliocene equatorial temperature: Lessons from atmospheric superrotation. *Paleoceanography*, *24*(1), PA1101. https://doi.org/10.1029/2008pa001652

Velasco-de León, M. P., Spicer, R. A., & Steart, D. C. (2010). Climatic reconstruction of two Pliocene floras from Mexico. *Palaeobiodiversity and Palaeoenvironments*, *90*(2), 99–110. https://doi.org/10.1007/s12549-010-0022-4

Vignaud, P., Duringer, P., Mackaye, H. T., Likius, A., Blondel, C., Boisserie, J.-R., et al. (2002). Geology and palaeontology of the Upper Miocene Toros-Menalla hominid locality, Chad. *Nature*, *418*(6894), 152–155. https://doi.org/10.1038/nature00880

Wara, M. W., Ravelo, A. C., & Delaney, M. L. (2005). Permanent El Niño-like conditions during the Pliocene warm period. *Science*, *309*(5735), 758–761. https://doi.org/10.1126/science.1112596

Wilkerson, F. P., Lassiter, A. M., Dugdale, R. C., Marchi, A., & Hogue, V. E. (2006). The phytoplankton bloom response to wind events and upwelled nutrients during the CoOP WEST study. *Deep Sea Research Part II: Topical Studies in Oceanography*, *53*(25–26), 3023–3048. https://doi.org/10.1016/j.dsr2.2006.07.007

Winnick, M. J., Welker, J. M., & Chamberlain, C. P. (2013). Stable isotopic evidence of El Niño-like atmospheric circulation in the Pliocene western United States. *Climate of the Past*, *9*(2). https://doi.org/10.5194/cp-9-903-2013

Wolfe, J. (1990). Estimates of Pliocene precipitation and temperature based on multivariate analysis of leaf physiognomy. In L. B. Gosnell, & R. Z. Poore (Eds.), *Pliocene Climates: Scenario for Global Warming* (Vol. 90–64). US Geological Survey Open-File Report.

Wycech, J. B., Gill, E., Rajagopalan, B., Marchitto, T. M., Jr, & Molnar, P. H. (2020). Multiproxy reduced-dimension reconstruction of Pliocene equatorial Pacific sea surface temperatures. *Paleoceanography and Paleoclimatology*, *35*(1), e2019PA003685. https://doi.org/10.1029/2019pa003685

Zazzo, A., Bocherens, H., Billiou, D., Mariotti, A., Brunet, M., Vignaud, P., et al. (2000). Herbivore paleodiet and paleoenvironmental changes in Chad during the Pliocene using stable isotope ratios of tooth enamel carbonate. *Paleobiology*, *26*(2), 294–309. https://doi.org/10.1666/0094-8373(2000)026<0294:hpapci>2.0.co;2

Zhang, Y. G., Pagani, M., & Liu, Z. (2014). A 12-million-year temperature history of the tropical Pacific Ocean. *Science*, *344*(6179), 84–87. https://doi.org/10.1126/science.1246172

References From the Supporting Information

Adam, D. P., Bradbury, J. P., Rieck, H. J., & Sarna-Wojcicki, A. (1990). Environmental changes in the Tule Lake Basin, Siskiyou and Modoc Counties, California, from 3 to 2 million years before present. *U.S. Geological Survey Bulletin*, 1–13.1933

Adam, D. P., Sarna-Wojcicki, A. M., Rieck, H. J., Bradbury, J. P., Dean, W. E., & Forester, R. M. (1989). Tulelake, California: the last 3 million years. *Palaeogeography, Palaeoclimatology, Palaeoecology*, *72*, 89–103.